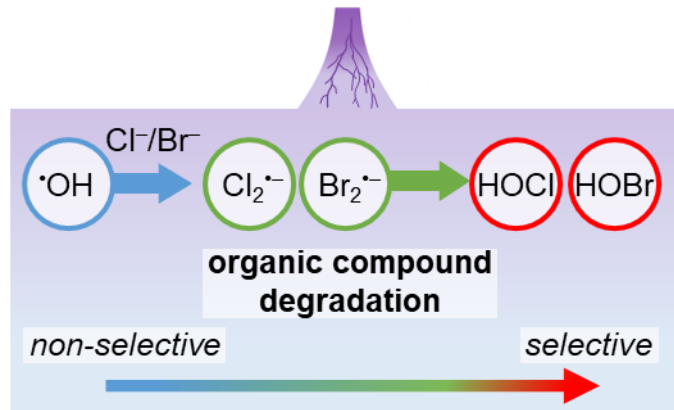


13 TOC Art



14

15 **Abstract**

16 Plasma has been proposed as an alternative strategy to treat organic contaminants in brines.
17 Chemical degradation in these systems is expected to be partially driven by halogen oxidants, which have
18 been detected in halide-containing solutions exposed to plasma. In this study, we characterized specific
19 mechanisms involving the formation and reactions of halogen oxidants during plasma treatment. We first
20 demonstrated that addition of halides accelerated the degradation of a probe compound known to react
21 quickly with halogen oxidants (i.e., *para*-hydroxybenzoate), but did not affect the degradation of a less
22 reactive probe compound (i.e., benzoate). This effect was attributed to the degradation of *para*-
23 hydroxybenzoate by hypohalous acids, which were produced via a mechanism involving halogen radicals
24 as intermediates. We applied this mechanistic insight to investigate the impact of constituents in brines on
25 reactions driven by halogen oxidants during plasma treatment. Bromide, which is expected alongside
26 chloride in brines, was required to enable halogen oxidant formation, consistent with the generation of
27 halogen radicals from the oxidation of halides by hydroxyl radicals. Other constituents typically present in
28 brines (i.e., carbonates, organic matter) slowed the degradation of organic compounds, consistent with their
29 ability to scavenge species involved during plasma treatment.

30 **Synopsis**

31 In plasma-based water treatment, halides lead to hypohalous acid formation via a radical-mediated pathway,
32 which contributes to the accelerated degradation of certain organic compounds.

33 **Keywords**

34 Brine treatment, plasma, halides, hypohalous acids, halogen radicals.

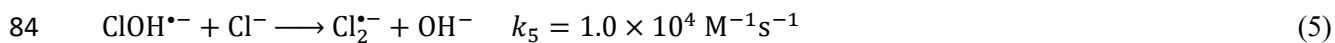
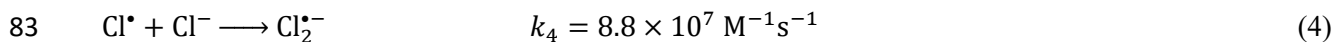
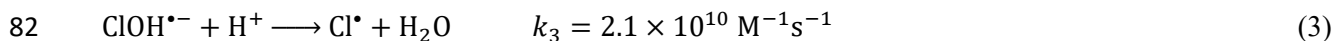
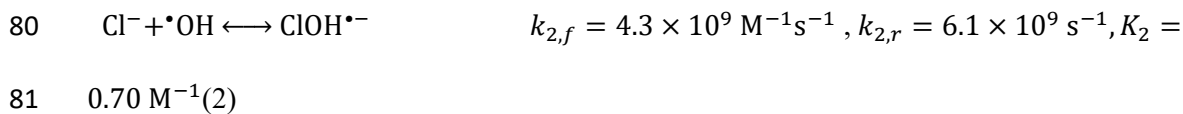
35 Introduction

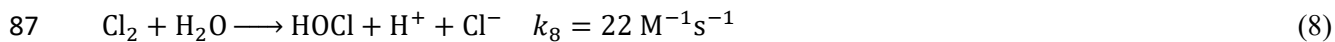
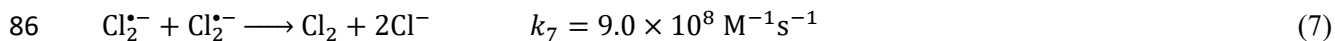
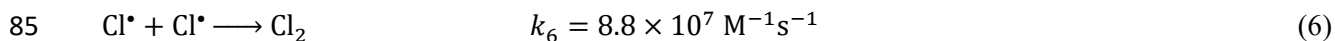
36 Plasma technology has been recently proposed as a promising tool for water treatment due to its
37 simplicity, cost, and effectiveness toward destroying toxic organic compounds.¹⁻⁷ Unlike
38 ultraviolet/oxidant advanced oxidation processes (UV/oxidant AOPs), plasma operates without requiring
39 chemical consumables (e.g., hydrogen peroxide, H₂O₂; hypochlorous acid, HOCl).⁵ In addition, though the
40 energy requirement may be substantial, plasma treatment of some organic contaminants has been reported
41 to be competitive against other treatment options including UV/oxidant AOPs, electrochemical treatment,
42 and sonolysis.^{6,7} Plasma-based water treatment generates an array of oxidative species (e.g., hydroxyl
43 radical, [•]OH; oxygen atom, O; ozone, O₃; hydrogen peroxide, H₂O₂)⁸⁻¹¹ via processes in the plasma or at
44 the plasma-water interface,^{4,8} among which [•]OH – known to react with a wide spectrum of organic
45 contaminants¹² – is frequently determined to drive the degradation of several organic contaminants (e.g.,
46 pesticides,¹³⁻¹⁵ pharmaceuticals,^{16,17} algal toxins¹⁸⁻²⁰). Plasma also generates reductive species (i.e.,
47 hydrated electron, e_{aq}⁻,²¹⁻²⁴ or its conjugate acid hydrogen atom, H[•],^{8,25} pK_a 9.6¹²) that degrade contaminants
48 such as per- and polyfluoroalkyl substances and halogenated disinfection byproducts in plasma^{7,26,27} or other
49 treatment technologies.²⁸⁻³³

50 Among possible applications, plasma has particular advantages when applied to degrade organic
51 compounds in brines. Contaminated brines encompass a wide array of waste streams from diverse sources
52 (ion exchange,^{34,35} reverse osmosis,³⁶⁻³⁸ pharmaceutical production,³⁹ hydraulic fracturing,^{40,41} landfill,⁴²
53 textile manufacturing⁴³), but all share high concentrations of salts and other constituents that present
54 multiple opportunities for plasma treatment. Firstly, relative to conventional AOPs, plasma appears to be
55 less susceptible to inhibition by constituents in complex wastewaters that scavenge reactive species.^{38,44} For
56 example, organic compound degradation by plasma was observed to be less sensitive to the inclusion of co-
57 occurring constituents in complex mixtures (i.e., reverse osmosis brine,³⁸ urine⁴⁴) compared to [•]OH-based
58 AOPs. Secondly, because reactive species are concentrated at or above the plasma-water interface,⁸ salting-
59 out effects in brines can improve the degradation efficiency of some contaminants (i.e., surfactants).⁴⁵ For

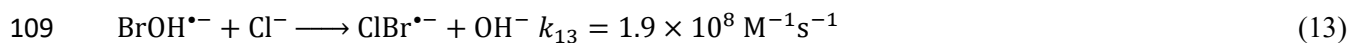
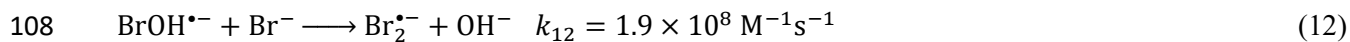
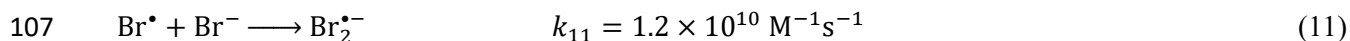
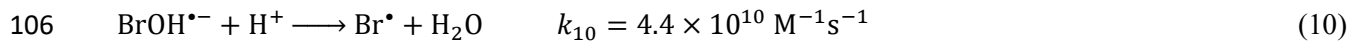
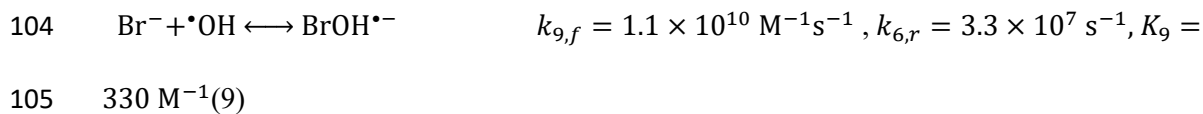
60 example, the degradation of perfluorooctanoic acid (PFOA), which is known to occur at or above the
 61 plasma-water interface,²⁶ was accelerated upon the addition of salts,⁴⁵ consistent with salts causing PFOA
 62 to more favorably partition to the water surface.⁴⁶⁻⁴⁸ Thirdly, increased conductivity at elevated salt
 63 concentrations affects plasma properties such as plasma volume and the contact area between plasma and
 64 water.⁴⁹ These changes can increase the production of reactive species (e.g., $\cdot\text{OH}$),⁵⁰ though notably the
 65 opposite trend has been observed in other reactors.^{44,49} Depending on the impact of conductivity on reactive
 66 species production in the specific reactor, the addition of salts has been reported to either accelerate^{51,52} or
 67 decelerate^{45,53,54} the degradation of organic compounds during plasma treatment.

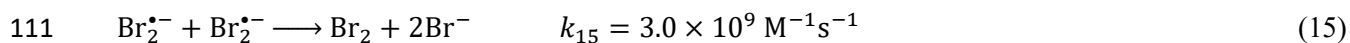
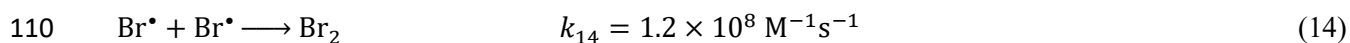
68 Beyond these contributions, halides present in brines may specifically enable new pathways due to
 69 their potential to form halogen oxidants during plasma treatment. For example, studies have invoked
 70 halogen oxidants, including HOCl and halogen radicals (i.e., $\text{Cl}\cdot$, $\text{Cl}_2^{\cdot-}$, $\text{ClOH}^{\cdot-}$), to explain compound
 71 degradation during plasma treatment of solutions containing chloride (Cl^-).^{45,54-56} HOCl has been measured
 72 to occur in Cl^- -containing solutions treated by plasma.⁵⁷⁻⁵⁹ The specific mechanisms proposed to be
 73 responsible for halogen oxidant formation depend on the plasma reactor setup. The inclusion of oxygen
 74 (i.e., at 0.1-1%) in the feed gas of some plasma systems enabled the generation of OCl^- , the conjugate base
 75 of HOCl, via the reaction between O and Cl^- (eq 1).⁵⁷⁻⁵⁹ In other plasma systems, an alternative mechanism
 76 involving the reaction between $\cdot\text{OH}$ and Cl^- (eq 2) to form $\text{Cl}\cdot$ (eq 3) and $\text{Cl}_2^{\cdot-}$ (eq 4-5) has been proposed
 77 in multiple studies,^{45,54-56} which may either react with organic compounds themselves^{54,56} or recombine to
 78 form HOCl (eq 6-8)⁶⁰⁻⁶² that drives compound degradation (**Table S1**).^{45,54,55}





88 These studies characterizing halogen oxidants in plasma-treated water have only investigated the
 89 impact of Cl^- ,^{45,54-59} which cannot account for the unique roles of other chemical species occurring in brines.
 90 In particular, brines, like natural waters,⁶³ also contain some bromide (Br^-) typically present at 0.1-1 mol
 91 percent of Cl^- ,^{41,64,65} which is particularly relevant for mechanisms involving halogen radicals.⁶⁶ Whereas
 92 HOCl formation from O can proceed in Cl^- -only systems,⁵⁷⁻⁵⁹ the presence of Br^- (even a trace contaminant
 93 in Cl^- reagent)^{67,68} is known to dominate the oxidation of halides by $\cdot\text{OH}$, leading to Br-containing halogen
 94 radicals (eq 9-13) and their recombination products (e.g., hypobromous acid, HOBr, eq 14-16, **Table S1**).⁶⁶
 95 Specifically, Cl^- itself is ineffective in scavenging $\cdot\text{OH}$ to produce halogen radicals due to the fast reverse
 96 reaction of the intermediate $\text{ClOH}^{\bullet-}$ to regenerate the initial reactants (eq 2),⁶⁶ whereas $\text{BrOH}^{\bullet-}$ generated in
 97 the presence of Br^- (eq 9) predominantly reacts further to produce halogen radicals (eq 10-13, e.g., >99.99%
 98 of $\text{ClOH}^{\bullet-}$ regenerates the reactants⁶⁹⁻⁷¹ compared to 14% of $\text{BrOH}^{\bullet-}$,⁷²⁻⁷⁴ **Text S1**).⁶⁶ Therefore, the
 99 previously proposed mechanism involving halogen radical formation in Cl^- -only systems treated by
 100 plasma^{45,54-56} has been typically considered negligible in other contexts (e.g., conventional AOPs).⁶⁶
 101 Beyond the effect of Br^- , other brine constituents (i.e., carbonates, organic matter) may also impact the
 102 formation and reactions of halogen oxidants during plasma treatment depending on the specific reactive
 103 species involved.^{64,67,68,75}





113 In this study, we evaluated the role of the halogen oxidants during plasma treatment of halide-
114 containing waters to incorporate consideration of Br^- and other constituents (i.e., carbonates, organic matter)
115 occurring in brines alongside Cl^- . We specifically focused on the formation of halogen oxidants mediated
116 by halogen radicals (eq 2-16) rather than O (eq 1) because we anticipated the inclusion of Br^- would play a
117 key role in this mechanism. To this end, we measured the degradation of probe compounds to provide
118 insight into the formation of halogen oxidants in solutions of different chemistries, as well as to evaluate
119 whether halogen radicals reacted with these compounds directly or recombined to form hypohalous acids
120 (**Table S1**)^{60-62,73,76-80} that drove the reaction instead. We complemented our experiments with
121 characterization of reactive species in plasma over solutions with and without halides. We applied our
122 mechanistic insight to evaluate organic compound degradation in the presence of brine constituents,
123 including known competitors for radicals (i.e., carbonates, organic matter).^{64,67,68} Overall, our work enables
124 the formation mechanism and reactions of halogen oxidants to be accurately understood in the presence of
125 key additional constituents beyond Cl^- during plasma treatment of contaminated brines.

126 **Materials and Methods**

127 **Reagents.** All chemicals used in this work are listed in Supporting Information, **Table S2**. All
128 experimental solutions were prepared in Milli-Q water. Stock solutions of HOCl and HOBr (~ 1.5-1.6 mM)
129 were prepared from sodium hypochlorite (5-6%) directly or by reacting with a stoichiometric amount of
130 Br^- and standardized spectrophotometrically at 292 nm⁸¹ or 329 nm,⁸² respectively.

131 **Plasma Reactor Setup.** The plasma reactor consisted of a flask with two electrodes and a high-
132 voltage power supply, as detailed in **Text S2** and **Figure S1**. To control headspace pressure and gas
133 composition, the flask was connected to a gas port equipped with a vacuum pump and a gas inlet. An ice
134 bath (4 °C) and a vapor condenser were used to minimize water loss during plasma treatment, which was

135 confirmed to be negligible (**Figure S2**). Exposure to plasma was found to promote internal mixing (**Figure**
136 **S3**), such that mechanical mixing (e.g., a stir bar) was not required. We omitted components required for
137 stirring to avoid additional complexities in the reactor design. Salts found to be deposited on the electrode
138 after plasma treatment of halide-containing solutions were analyzed for composition using a scanning
139 electron microscope (Thermo Fisher Scientific).

140 We used 99.999% argon (Linde Gas & Equipment Inc.) as the feed gas in our system. Argon was
141 selected to achieve a high plasma density (i.e., relative to helium)⁸³ and avoid the formation of reactive
142 nitrogen species (as opposed to nitrogen gas or air).¹⁴ The absence of oxygen in the feed gas is consistent
143 with feed gas compositions previously shown to lead to negligible hypohalous acid formation mediated by
144 O (eq 1),⁵⁹ consistent with our goal to investigate pathways mediated by halogen radicals (eq 2-16). While
145 O-mediated hypohalous acid formation is negligible without oxygen in the feed gas (i.e., <2 ppm_v, **Table**
146 **S2**), some O may be generated due to the presence of lower amounts of oxygen from other sources (e.g.,
147 ambient air, residual air, oxygen impurity in feed gas).⁸⁴ Trace oxygen may also scavenge electrons,⁸⁵ but
148 this effect is not expected to be relevant to the processes studied herein.

149 **Treatment of Solutions by Plasma.** To investigate the mechanism of how halides contributed to
150 organic compound degradation, two probe compounds (i.e., benzoate and *para*-hydroxybenzoate) were
151 used during plasma treatment. Solutions (50 mL) were prepared with 10 mM phosphate buffer (pH 7), 50
152 μM of each probe compound, and halides at indicated concentrations. In experiments containing both Br⁻
153 and Cl⁻, Br⁻ was added at 1 mol percent of Cl⁻, corresponding to molar ratios reported in brines (i.e., 0.1-
154 1 mol percent, **Table S3**).^{35,39,41,42,64,65,86-111} When isolating the effect of Cl⁻ alone, different experiments
155 were performed with both lower purity (i.e., ≥99.0%, 0.004 mol percent Br⁻, **Text S3**,^{67,112} **Figure S4**) and
156 higher purity (99.999%) Cl⁻ reagents as indicated in corresponding figures. When Br⁻ was added, the lower
157 purity Cl⁻ was used because the trace Br⁻ in the Cl⁻ reagent is negligible relative to the added Br⁻.
158 Perchlorate (ClO₄⁻) was used as a control for ionic strength. Because conductivity affects reactive species
159 production during plasma exposure,^{44,49,50} we confirmed that halide- and ClO₄⁻-containing solutions at the

160 same ionic strength had comparable solution conductivity (**Figure S5**). Consequently, controls for ionic
161 strength using ClO_4^- also served to control solution conductivity. Isopropanol (50 mM) was added in
162 specific experiments as a scavenger for radicals.

163 Prior to all experiments, the system was held at a low pressure (i.e., 25 Torr) for 5 min to degas
164 solutions. Then, the flask headspace was purged three times before filling with argon at 100 Torr. This
165 subatmospheric pressure was selected to achieve greater radical density during plasma treatment.¹¹³ We
166 confirmed that the degradation of probe compounds at 100 Torr was faster than at atmospheric pressure
167 (i.e., 760 Torr) in both halide- and ClO_4^- -containing solutions and that the effect of halides was consistent
168 at both pressures (**Figure S6**). After exposure to plasma at indicated times, aliquots (each 0.5 mL) were
169 collected by a syringe through a septum. Then, each aliquot was transferred to a 2 mL amber vial, quenched
170 by 5 μL 0.1 M ascorbic acid, and analyzed for probe compound concentrations. Concentrations of
171 hypohalous acids were measured by sampling 2 mL aliquots either at the end of the experiment (if a single
172 concentration was determined) or at multiple time points in experiments separate from probe compound
173 measurements. All sampling removed <24% of overall solution volume over the experiment duration.

174 Additional experiments were performed by further modifying the solution composition. In addition
175 to the probe compounds used above, four organic contaminants (i.e., salicylate, acetaminophen,
176 sulfamethoxazole, anthranilate) were selected based on their different reactivities toward halogen oxidants
177 (**Table S4**).^{62,77,114–119} Like Cl^- and Br^- , additional constituents (i.e., sulfate, SO_4^{2-} ; nitrate, NO_3^- ; carbonates;
178 organic matter) were added at brine-relevant concentrations (**Table S3**).^{35,39,41,42,64,65,86–111} Some of these
179 constituents have known reactivities with the reactive species of interest (**Table S5**).^{12,64,75,120–128} All salts
180 used in this study contained sodium as the cation. While calcium and magnesium were present in some
181 brines (**Table S3**),^{35,39,41,42,64,65,86–111} these cations were excluded from the present study to avoid
182 precipitation of solids with some anions (i.e., SO_4^{2-} , carbonates).^{129–131} When included, carbonates were
183 introduced to the solution using a syringe after the headspace was filled with argon to prevent loss of
184 carbonates as carbon dioxide during degassing. The ionic strength of all solutions was adjusted to a constant
185 value (2.0 M) using ClO_4^- .

186 **Analysis of Dissolved Species.** The summed concentrations of hypohalous acids (i.e., HOCl,
187 HOBr) were measured by the N,N-diethyl-phenylenediamine (DPD) colorimetric method¹³² using a
188 UV–vis spectrophotometer (Varian Cary) or Nanodrop (Thermo Fisher Scientific). The total concentrations
189 of hypohalous acids were calculated by standard curves for HOCl or HOBr, which were found to be
190 identical (**Figure S7**). The concentrations of organic compounds were quantified on an Agilent 1260
191 Infinity II High Pressure Liquid Chromatography – UV as described in **Text S4**. The retention times, UV
192 wavelengths, and the limits of detection (LOD) of organic compounds were reported in **Table S6**.

193 **Analysis of Species in Plasma by Optical Emission Spectroscopy (OES).** To investigate reactive
194 species present in plasma over solutions of different chemistries, analysis using two different OES
195 spectrometers was carried out using a glass vessel with optical windows (quartz) as a custom feature made
196 in Department of Chemistry at Washington University in St. Louis (modified from the aforementioned
197 reactor design as shown in **Figure S1**). Firstly, a low-resolution OES spectrometer (Ocean Optics HR4000
198 CG-UV-NIR) was used to obtain broadband OES spectra (i.e., 200-1100 nm) to identify species with strong
199 emission intensities in plasma. Secondly, a high-resolution OES spectrometer (Princeton Instrument
200 SpectraPro HRS-750) was used over narrow ranges of wavelengths to observe species with weak emission
201 intensities. The identification of species by each OES spectrometer was achieved by comparing
202 wavelengths to those reported previously (**Table S7**).^{133–136} While OES provides information about the
203 presence of observable species, it does not directly provide information about species concentrations in
204 plasma.

205 **Statistical Analysis.** All experiments were conducted in duplicate. Errors in concentrations
206 represent the range of measurements from duplicate experiments, while errors in degradation rate constants
207 and rates represent the standard errors of the slopes obtained from linear regression. The significance of
208 differences was evaluated using GraphPad Prism with a confidence level set to be ≤ 0.05 .

209 **Results and Discussion**

210 **Effects of Halides on Probe Compound Degradation.** We first evaluated whether halogen
211 oxidants were generated during plasma treatment of solutions containing mixed halides (i.e., 1 M Cl⁻ along
212 with 10 mM Br⁻). In addition to the chlorine-relevant species (i.e., Cl[•], Cl₂^{•-}, HOCl) invoked in prior
213 studies,^{45,54-56} Br⁻ is also expected to enable the formation of bromine-relevant radicals (i.e., Br[•], Br₂^{•-}),
214 mixed halogen radicals (i.e., ClBr^{•-}), and HOBr.⁶⁶ To this end, we compared the degradation rates of two
215 probe compounds, benzoate and *para*-hydroxybenzoate, selected due to their reported bimolecular rate
216 constants with both chlorine and bromine species (**Table S4**).^{62,77,114-117} In the absence of halides, both probe
217 compounds are expected to degrade at similar rates due to their similar rate constants for reactions with
218 common species generated by plasma (e.g., [•]OH, e_{aq}⁻, H[•], **Table S4**).¹³⁷⁻¹⁴¹ In contrast, if halogen oxidants
219 are formed in the presence of halides, *para*-hydroxybenzoate is expected to degrade more quickly than
220 benzoate, corresponding to its substantially higher bimolecular rate constants with both halogen radicals¹¹⁵⁻
221 ¹¹⁷ and hypohalous acids.^{62,114}

222 In the absence of halides, benzoate and *para*-hydroxybenzoate degraded at similar rates in a
223 solution with 1 M ClO₄⁻ added to increase ionic strength (**Figure 1a**). Consistent with the reported kinetics
224 of other organic compounds treated by plasma,^{7,13,15,26,30,44} the degradation of both compounds followed
225 pseudo-first-order kinetics, resulting in rate constants of 0.0121±0.0007 min⁻¹ and 0.0108±0.0006 min⁻¹ for
226 the degradation of benzoate and *para*-hydroxybenzoate, respectively (**Figure 1a**). To determine the effect
227 of ionic strength in our reactor, we measured probe compound degradation in solutions without ClO₄⁻,
228 finding that each rate constant increased by 40-50% (i.e., to 0.017±0.001 min⁻¹ for benzoate and
229 0.016±0.001 min⁻¹ for *para*-hydroxybenzoate (**Figure S8**). This result suggests that ionic strength and
230 conductivity in our reactor slightly suppresses probe compound degradation, but that reactive species with
231 comparable reactivities towards both compounds (i.e., [•]OH, **Table S4**)^{137,138} dominate the reaction
232 regardless of ionic strength.

233 Consistent with our hypothesis, the addition of halides (i.e., 1 M Cl⁻, 10 mM Br⁻) marginally
234 affected benzoate degradation (**Figure 1b**), but accelerated *para*-hydroxybenzoate degradation (**Figure 1c**).
235 However, before proceeding with quantitative analysis of these effects, we were first required to address

236 our observation that the kinetics of *para*-hydroxybenzoate degradation in the presence of halides appeared
237 to deviate from pseudo-first-order (**Figure 1c**). Additional residual analysis supported our observation that,
238 unlike the probe compound degradation in the presence of ClO_4^- , *para*-hydroxybenzoate degradation in the
239 presence of halides more closely followed zero-order kinetics (**Figure S9**). Because benzoate was degraded
240 by <20% over the same time frame in the presence of halides, analysis of the reaction order was not
241 attempted. To facilitate comparisons among probe compound degradation in different chemistries that alter
242 reaction order, we opted to report observed zero-order degradation rates of each compound during the first
243 30 min of exposure to plasma (**Figure 1b,c**). Using this approach, we determined that the degradation rate
244 of benzoate was not significantly impacted by replacing ClO_4^- with halides, while the degradation rate of
245 *para*-hydroxybenzoate was selectively increased 3-fold.

246 In addition to affecting our quantitative analysis, the degradation of *para*-hydroxybenzoate by
247 observed zero-order kinetics also enabled us to evaluate the potential for each class of halogen oxidants
248 (i.e., halogen radicals or hypohalous acids) to contribute directly (i.e., as opposed to acting as intermediates)
249 to the accelerated rate in the presence of halides. If halogen radicals directly reacted with *para*-
250 hydroxybenzoate, we expected that the reaction would follow pseudo-first-order kinetics, consistent with
251 organic compound degradation in UV/oxidant AOP treatment of halide-containing waters.^{67,68,142} Therefore,
252 we instead hypothesized that hypohalous acids, which form from the recombination of radical species,⁶⁶
253 react with *para*-hydroxybenzoate. Our hypothesis was based on the observation that the overall
254 concentration of hypohalous acids – both in the absence and presence of probe compounds – increased as
255 the solution exposure to plasma increased (**Figure 1d**), which might allow the reaction rate to be maintained
256 even as *para*-hydroxybenzoate concentration diminished.

257 To determine if the increasing amount of hypohalous acids was quantitatively consistent with the
258 observed zero-order kinetics of *para*-hydroxybenzoate, we analyzed the instantaneous rate of *para*-
259 hydroxybenzoate loss at each time point using the equation:

$$260 \quad -d[\text{C}]/dt = k_{\text{C,HOCl}}[\text{HOCl}][\text{C}] + k_{\text{C,HOBr}}[\text{HOBr}][\text{C}] \quad (17)$$

261 where [C] represents the measured concentration of *para*-hydroxybenzoate (**Figure 1c** in the presence of
262 halides); t represents the duration of exposure to plasma; $k_{C,HOCl}$ and $k_{C,HOBr}$ represent the apparent
263 bimolecular rate constant between *para*-hydroxybenzoate and each hypohalous acid (either found in or
264 estimated from literature, **Text S5, Table S4**);^{77,114} and [HOCl] and [HOBr] represent the concentrations of
265 HOCl and HOBr. Reactions involving the conjugate bases of HOCl and HOBr were assumed to be
266 negligible due to both their lower concentrations at the experimental pH and their slower reactivities toward
267 substituted aromatics.^{77,143}

268 To further simplify this equation, we defined the term f_{HOCl} as the fraction of hypohalous acid
269 present as HOCl (i.e., $f_{HOCl} = [HOCl]/[HOX]_{tot}$, where $[HOX]_{tot}$ is the total concentration of hypohalous
270 acids). Then, [HOCl] and [HOBr] in eq 17 were substituted with $f_{HOCl}[HOX]_{tot}$ and $(1 - f_{HOCl})[HOX]_{tot}$,
271 respectively, to generate:

$$272 \quad -d[C]/dt = [k_{C,HOCl}f_{HOCl} + k_{C,HOBr}(1 - f_{HOCl})][HOX]_{tot}[C] \quad (18)$$

273 Due to the constant pH and near-constant concentrations of Cl^- and Br^- , f_{HOCl} is expected to be
274 approximately constant during the experiment.⁷⁷ Consequently, *para*-hydroxybenzoate is calculated to
275 degrade upon reactions with hypohalous acids following observed zero-order kinetics (i.e., $d[C]/dt$ is
276 constant), if the multiplication product of the concentrations of *para*-hydroxybenzoate and total hypohalous
277 acids (i.e., $[HOX]_{tot}[C]$) is near-constant. When we calculated this term using experimental concentrations
278 of *para*-hydroxybenzoate (**Figure 1c**, condition: with halides) and hypohalous acids (**Figure 1d**, condition:
279 with probe compounds), we found that the value of $[HOX]_{tot}[C]$ did not vary during the experimental period
280 (i.e., slope of $0 \pm 2 \mu M^2/min$, **Figure S10**), consistent with the observed zero-order kinetics of *para*-
281 hydroxybenzoate degradation.

282 In addition to confirming that measured hypohalous acid concentrations were consistent with the
283 observed reaction order, we also evaluated if the amount of hypohalous acids measured in our system could
284 feasibly account for the observed rate of *para*-hydroxybenzoate degradation using bimolecular rate
285 constants available or estimated from literature.^{77,114} Assuming all hypohalous acid was present as HOCl

286 (i.e., $f_{\text{HOCl}} = 1$), the calculated *para*-hydroxybenzoate degradation rate (i.e., $0.22 \pm 0.09 \mu\text{M}/\text{min}$, **Figure**
287 **S11**) is lower than but within the same order of magnitude as the measured rate (i.e., $1.36 \pm 0.07 \mu\text{M}/\text{min}$,
288 **Figure 1c**). Conversely, if HOBr is assumed to be exclusively present (i.e., $f_{\text{HOCl}} = 0$), the calculated rate
289 (i.e., $900 \pm 400 \mu\text{M}/\text{min}$, **Figure S11**) is >2 orders of magnitude higher than the measured rate. Because
290 HOBr has been modeled to occur at higher concentrations than HOCl in seawater containing 0.0015 mol-
291 $\text{Br}^-/\text{mol-Cl}^-$,¹⁴⁴ HOBr is expected to also dominate in our system, which has both higher halide
292 concentrations and Br^-/Cl^- ratio. Consequently, our measured $[\text{HOX}]_{\text{tot}}$, if present primarily as HOBr,
293 overpredicts the observed degradation rate of *para*-hydroxybenzoate, possibly due to an overestimation of
294 the bimolecular rate constant between *para*-hydroxybenzoate and HOBr (**Table S4**). Recently, reactions
295 with organic compounds involving previously overlooked species (e.g., Br_2O , Br_2) have been found to
296 contribute to rate constants for reactions attributed to HOBr being overestimated by similar orders of
297 magnitude.^{145,146} While re-evaluation of this bimolecular rate constant is beyond the scope of this work, our
298 analysis with currently available values suggests that hypohalous acids are present at sufficient
299 concentrations, if not in excess, to account for the observed rate of *para*-hydroxybenzoate degradation.

300 While our results are consistent with hypohalous acids acting as the primary species directly
301 reacting with *para*-hydroxybenzoate to accelerate its degradation in the presence of halides, we still
302 hypothesized that radicals (i.e., $\cdot\text{OH}$, halogen radicals) act as intermediates that go on to form hypohalous
303 acids via recombination reactions.⁶⁶ To test this hypothesis, we repeated our experiments in solutions
304 including 50 mM isopropanol, a known scavenger of both $\cdot\text{OH}$ (i.e., $k_{\text{isopropanol},\cdot\text{OH}} = 1.9 \times$
305 $10^9 \text{ M}^{-1}\text{s}^{-1}$)¹² and halogen radicals (i.e., $k_{\text{isopropanol},\text{Cl}_2\cdot^-} = 1.2 \times 10^5 \text{ M}^{-1}\text{s}^{-1}$,¹¹⁵ $k_{\text{isopropanol},\text{Br}\cdot} =$
306 $6.6 \times 10^6 \text{ M}^{-1}\text{s}^{-1}$).⁷³ In addition, isopropanol is not expected to quench hypohalous acids directly due to
307 slow reported rate constants (e.g., $k_{\text{isopropanol},\text{HOBr}} < 3.9 \times 10^{-4} \text{ M}^{-1}\text{s}^{-1}$),¹⁴⁷ which we confirmed by
308 demonstrating that isopropanol did not impact *para*-hydroxybenzoate degradation by hypohalous acids
309 added directly as HOCl to halide-containing solutions (**Figure S12**). The addition of isopropanol to halide-
310 containing solutions decreased the degradation rate of *para*-hydroxybenzoate to $0.20 \pm 0.02 \mu\text{M}/\text{min}$, which

311 was 6-fold lower than the rate measured in halide-containing solutions without isopropanol (**Figure 1c**).
312 Consistent with our proposed pathway of hypohalous acid formation from radical recombination, we
313 determined that the addition of isopropanol reduced the concentration of hypohalous acids after plasma
314 treatment to below their LOD (**Figure S13**).

315 The above evidence supports our expectation that our plasma system generates hypohalous acids
316 through a radical-mediated pathway (i.e., recombination of halogen radicals formed from halide oxidation
317 by $\cdot\text{OH}$) in solutions containing Cl^- and Br^- together. This pathway has been invoked previously to explain
318 results obtained during plasma treatment of solutions containing Cl^- as the sole halide,^{45,54-56} which
319 contradicts prior work that suggests Cl^- oxidation by $\cdot\text{OH}$ is negligible.⁶⁶ This discrepancy was possibly
320 due to a trace amount of Br^- impurity occurring in the Cl^- reagent, which has previously been implicated in
321 halogen radical formation.^{67,68} We found that the inclusion of 1 M Cl^- added as a low purity reagent (i.e.,
322 $\geq 99.0\%$ with 0.004 mol percent Br^-) increased the degradation rate of *para*-hydroxybenzoate by $22 \pm 9\%$
323 relative to the ionic strength control ($p=0.02$, **Figures 1e**). In contrast, the inclusion of 1 M Cl^- added as a
324 high purity reagent (i.e., 99.999%) did not increase the rate relative to the control (**Figure 1e**). Similarly,
325 hypohalous acid concentrations after treatment for 30 min were measurable in solutions prepared with low
326 purity Cl^- (i.e., $4.2 \pm 0.8 \mu\text{M}$), but below the LOD (i.e., $0.8 \mu\text{M}$) in solutions prepared with either ClO_4^- or
327 high purity Cl^- (**Figure 1e**). These results suggest that plasma treatment of solutions containing Cl^- as the
328 sole halide is unlikely to generate hypohalous acids via a radical-mediated pathway, as well as indicate that
329 a trace amount of Br^- impurity, which varies in magnitude among Cl^- reagents, may contribute to some
330 effects previously attributed to Cl^- alone during plasma treatment.

331 While the effect of 1 mM Cl^- as the sole halide was negligible in our system, the inclusion of 10
332 mM Br^- (along with 1 M ClO_4^- to control the ionic strength) affected both compound degradation and
333 hypohalous acid formation to similar extents with or without 1 M Cl^- present (**Figure 1e**). The degradation
334 rate of *para*-hydroxybenzoate in the Br^- -only solution was $81 \pm 7\%$ of the rate when Br^- and Cl^- were present
335 together, and the concentration of hypohalous acid was indistinguishable between the two solutions after

336 30 min of exposure to plasma. In $\cdot\text{OH}$ -initiated pathways, lower concentrations of Br^- alone (i.e., 0.001-0.1
337 mM) have been previously reported to negligibly affect downstream reactions,^{142,148,149} whereas higher
338 concentrations of Br^- alone (i.e., 1 mM) accelerated organic compound degradation.¹⁴⁹ Consistent with
339 these findings, the elevated Br^- concentration used in our study (10 mM, corresponding to 1 mol percent
340 Cl^-) appears to be sufficient to account for the halide-dependent reactions in our plasma system regardless
341 of the presence of Cl^- .

342 Though the amount of Br^- relative to Cl^- is relatively consistent in brines (i.e., 0.1-1 mol percent
343 Br^- , **Table S3**), the absolute concentrations of halides vary substantially (e.g., 0.007-2 M Cl^- , **Table**
344 **S3**).^{35,39,41,42,64,65,86-111} Therefore, we expanded our experiments to evaluate the effect of halides at different
345 concentrations, but at a constant ratio of Br^- to Cl^- (i.e., 0.1-2 M Cl^- with 1 mol percent of Br^-). The inclusion
346 of halides at concentrations higher than 0.5 M Cl^- and 5 mM Br^- increased the degradation rate of *para*-
347 hydroxybenzoate by 2- to 4-fold relative to ClO_4^- at the same ionic strength and conductivity (**Figure 1f**).
348 We also observed hypohalous acid formation across all tested halide concentrations (**Figure 1f**). Both the
349 acceleration of *para*-hydroxybenzoate degradation and hypohalous acid formation increased to lesser
350 degrees upon increasing addition of halides at high concentrations, possibly due to other limitations (e.g.,
351 $\cdot\text{OH}$ generation by plasma).

352 **Effects of Halides on Reactive Species in Plasma.** We next investigated reactive species in plasma
353 using low- (**Figure S14**) or high-resolution OES (**Figures 2,S15**). Consistent with our proposed mechanism
354 to generate halogen oxidants from halide oxidation by $\cdot\text{OH}$ (eq 2-16), we detected the presence of $\cdot\text{OH}$ in
355 plasma by both the low-resolution and high-resolution OES above all solutions regardless of the presence
356 of halides or ionic strength (**Figures S14,15, Table S7**). Although our feed gas did not include oxygen in
357 amounts required to generate hypohalous acids from O (eq 1),⁵⁹ O was also detected by high-resolution
358 OES (**Figure 2k, Table S7**), though not by low-resolution OES (**Figure S14**). The presence of O in plasma
359 has been previously observed even when oxygen was not added in the feed gas.⁸⁴

360 The collected OES spectra also afforded us the opportunity to determine if halogen species (i.e.,
361 Cl^\cdot , Br^\cdot , as well as molecular halogens, i.e., Cl_2 , Br_2) could be detected in the plasma phase during treatment

362 of halide-containing solutions. In addition to their possible generation at the interface of the plasma and
363 liquid in our reactor,⁸ we also noticed evidence that halide-containing aerosols – which may allow
364 heterogeneous oxidation of halides by $\cdot\text{OH}$ at their interface^{150–152} – were generated in our system during
365 plasma treatment. Specifically, we noted salt deposition on the electrode after plasma treatment, which we
366 determined to be primarily composed of sodium chloride (**Figures S16,17**) likely transferred to the
367 electrode by aerosols generated during plasma exposure.⁸ Using low-resolution OES, we also observed a
368 large sodium (Na) peak above solutions containing either halides (i.e., 1 M Cl^- , 10 mM Br^-) or 1 M ClO_4^- ,
369 suggesting that salts in solutions may generate plasma species (**Figure S14**). However, no halogen species
370 were detected in the plasma regardless of the presence of halides (**Figure 2, Table S7**), suggesting either
371 that these species were present below their LOD (which could not be quantified for OES) or that halogen
372 oxidants were primarily confined to the liquid phase of the reactor.

373 **Effects of Brine Constituents on Organic Contaminant Degradation.** We expanded our
374 experiments to include four organic contaminants selected due to their reported bimolecular rate constants
375 toward hypohalous acids, which span orders of magnitude (**Table S4**).^{62,77,114,119} In the ionic strength control,
376 all contaminants degraded at rates comparable to the probe compounds (**Figure 3a**), in agreement with their
377 similar bimolecular rate constants toward species generated by plasma in the absence of halides (e.g., $\cdot\text{OH}$,
378 e_{aq}^- , **Table S4**).^{137–139,153–156} The addition of halides selectively accelerated the degradation of two
379 contaminants (i.e., sulfamethoxazole, anthranilate) to extents similar to or greater than *para*-
380 hydroxybenzoate (**Figure 3a**); like *para*-hydroxybenzoate, the accelerated degradation of these
381 contaminants (e.g., anthranilate) also followed zero-order kinetics (**Figure S18**). The acceleration of
382 degradation rates of the compounds upon halide addition correlated with their reactivity towards
383 hypohalous acids, which occurred at measurable concentrations (i.e., $35 \pm 5 \mu\text{M}$ after 30 min of exposure to
384 plasma, **Figure S19**). Specifically, the bimolecular rate constants for the reactions of five of the six
385 compounds with HOCl (available for all compounds, **Table S4**),^{62,114} which typically trend with rate
386 constants with HOBr⁷⁷ correlate with greater degradation rates (**Figure 3a**). The bimolecular rate constants
387 involving HOBr, which have only been reported for three of these compounds (**Table S4**),^{77,119} may explain

388 the one exception: acetaminophen, which did not undergo faster degradation upon halide addition despite
389 reacting with HOCl with a rate constant comparable to *para*-hydroxybenzoate,^{62,114} reacts more slowly with
390 HOBr (**Table S4**).^{77,119}

391 We next evaluated the impact of additional constituents reported to occur in brines (**Table**
392 **S3**)^{35,39,41,42,64,65,86–111} on the degradation of these compounds in the presence of halides, beginning with two
393 species – SO_4^{2-} and NO_3^- – not expected to affect our proposed pathway. Neither SO_4^{2-} nor NO_3^- scavenges
394 $\cdot\text{OH}$ (**Table S5**);^{122,123} though NO_3^- reacts with e_{aq}^- (**Table S5**),¹²⁶ e_{aq}^- is not invoked in the radical-mediated
395 generation of hypohalous acids. Consistent with our expectation, both degradation rates of organic
396 compounds (**Figure 3a**) and hypohalous acid concentrations (**Figure S19**) were comparable in the presence
397 of these anions at their median concentrations reported in brines (i.e., 0.25 M SO_4^{2-} , 0.08 M NO_3^- , **Table**
398 **S3**).^{35,39,41,42,64,65,86–111}

399 Among the four contaminants, we selected one exhibiting accelerated degradation in the presence
400 of halides and one not (sulfamethoxazole and acetaminophen, respectively) for additional experiments
401 involving brine constituents expected to impact our pathway, beginning with carbonates. Carbonates (i.e.,
402 bicarbonate, HCO_3^- ; carbonate, CO_3^{2-}) react with both $\cdot\text{OH}$ and halogen radicals to produce carbonate
403 radicals ($\text{CO}_3^{\cdot-}$, **Table S5**).^{12,120,121,124} $\text{CO}_3^{\cdot-}$ reacts rapidly with both contaminants (i.e.,
404 $k_{\text{acetaminophen},\text{CO}_3^{\cdot-}} = 1.9 \times 10^9 \text{ M}^{-1}\text{s}^{-1}$, $k_{\text{sulfamethoxazole},\text{CO}_3^{\cdot-}} = 4.4 \times 10^8 \text{ M}^{-1}\text{s}^{-1}$).¹⁵⁷ However, the
405 scavenging of halogen radicals by carbonates⁶⁸ is expected to reduce the formation of hypohalous acids,
406 which thereby suppresses resultant contaminant degradation. In the presence of halides without carbonates,
407 the degradation rates of both acetaminophen and sulfamethoxazole were 2-fold higher when isolated as a
408 pair of compounds (**Figure 3b**) than when present with the four other compounds (**Figure 3a**); this increase
409 is attributable to the reduced competition for reactive species that also lead to 1.5-fold higher hypohalous
410 acid concentration (i.e., 51 ± 2 after 30 min, **Figure S20**). While the addition of carbonates did not alter the
411 degradation rate of acetaminophen, the degradation rate of sulfamethoxazole was reduced by 6-fold when
412 carbonates were added at 0.16 M (**Figure 3b**). The addition of carbonates also reduced the formation of

413 hypohalous acids; their measured concentration decreased to $1.5 \pm 0.5 \mu\text{M}$ after solution exposure to plasma
414 for 30 min in the presence of 0.16 M carbonates (**Figure S20**).

415 Organic matter is another brine constituent expected to inhibit our proposed pathway due to its
416 known reactions with both radicals (e.g., $\cdot\text{OH}$, **Table S5**)^{64,125} and hypohalous acids (**Table S5**).⁷⁵ The
417 addition of organic matter (i.e., Aldrich humic acid, AHA; Suwannee River natural organic matter, SRNOM)
418 to halide-containing solutions did not impact the degradation of acetaminophen, but decreased the
419 degradation rate of sulfamethoxazole (**Figure 3c**). Relative to UV/oxidant AOPs, a higher concentration of
420 organic matter was required to suppress contaminant degradation to a comparable extent during plasma
421 treatment. For example, while the addition of organic matter at 100 mg-C/L only decreased the degradation
422 rate of sulfamethoxazole by 19-40% during plasma treatment (**Figure 3c**), the addition of organic matter at
423 a lower concentration (i.e., 36 mg-C/L) to saline waters decreased pharmaceutical degradation by 60-90%
424 during treatment by UV/oxidant AOPs.⁶⁴

425 **Environmental Implications.** In this work, we demonstrated that Br^- , despite only occurring in
426 low amounts relative to Cl^- in brines, plays a crucial role during plasma treatment of halide-containing
427 solutions. Our finding is consistent with prior work demonstrating that the generation of halogen radicals
428 via halide oxidation by $\cdot\text{OH}$ requires Br^- to be present along with Cl^- (**Table S1**).⁶⁶ The dependency of
429 halogen radical formation on the presence of Br^- may be harnessed in future applications to distinguish
430 hypohalous acid formation via halogen radicals from their formation mediated by O , which was reported
431 to require only Cl^- (eq 1),⁵⁷⁻⁵⁹ in plasma reactors wherein both pathways are feasible. In these applications,
432 the potential for trace Br^- occurring in Cl^- reagents to enable halogen radical formation must be considered,
433 as previously demonstrated for UV/oxidant AOPs.^{67,68} Furthermore, the unique role of Br^- must be
434 accounted for when translating prior studies on plasma treatment in Cl^- -only solutions^{45,54-56} to more
435 complex chemistries occurring in brines, as well as other halide-containing solutions (i.e., blood serum)¹⁵⁸
436 exposed to plasma.¹⁵⁹

437 Whereas the degradation of organic compounds in halide-containing solutions during UV/oxidant
438 AOP treatment is typically attributable to their reactions with halogen radicals,^{67,68,142} the plasma system is

439 unique because organic compounds are primarily degraded due to reactions with hypohalous acids, which
440 are generated by the recombination of halogen radicals.⁶⁶ A possible cause for this difference is that the
441 generation of radical species during plasma treatment primarily occurs at the plasma-water interface,⁸
442 potentially leading to localized regions of high radical concentrations that accelerates the recombination
443 reactions. Beyond determining the kinetics of compound degradation, the formation of hypohalous acids
444 during plasma treatment is relevant if applications of plasma for disinfection¹⁶⁰⁻¹⁶³ are expanded to systems
445 wherein halides are present. In addition, the formation of hypohalous acids potentially leads to the
446 generation of halogenated byproducts,^{164,165} though these byproducts may also undergo dehalogenation by
447 reductive species³¹⁻³³ generated by plasma.

448 By elucidating the distinct roles of both radicals and hypohalous acids in organic contaminant
449 degradation during plasma treatment of halide-containing waters, our work also informs more accurate
450 consideration of the impact of other brine constituents on these reactions. Only constituents with known
451 reactions with radicals and/or hypohalous acids (i.e., carbonates, organic matter, as opposed to SO_4^{2-} and
452 NO_3^-) suppressed contaminant degradation. The ability of carbonates to prevent hypohalous acid formation
453 by scavenging halogen radicals⁶⁸ appeared to dominate over the potential for CO_3^{2-} to itself contribute to
454 contaminant degradation,^{157,166} resulting in slower degradation rates. Hypohalous acids formed during
455 plasma treatment may also be less susceptible to scavenging by organic matter than radicals (**Table**
456 **S5**),^{64,75,125} contributing to smaller reductions in contaminant degradation than reported in UV/oxidant
457 AOPs.⁶⁴

458 Our results also impact approaches that enable plasma systems to be compared to other
459 technologies for brine treatment. A typical basis for comparison is energy consumption, which has been
460 quantified as the electrical energy required per order of magnitude compound degradation (E_{EO}) using
461 pseudo-first-order rate constants.¹⁶⁷ In the presence of ClO_4^- , we calculated the E_{EO} of probe compounds
462 based on their pseudo-first-order degradation rate constants (**Figure 1a**). Using the total power output (i.e.,
463 15 W) and the solution volume (i.e., 0.05 L), the E_{EO} for probe compounds ranged from 950-1,070 kWh/m^3
464 per order, which was within the same order of magnitude as previously reported E_{EO} for pharmaceutical

465 degradation during plasma treatment (i.e., 10^3 - 10^4 kWh/m³).⁴⁴ However, our results demonstrate that this
466 approach is unsuitable as a basis to compare plasma technologies – both among different plasma reactors
467 and to other treatment technologies, e.g., UV/oxidant AOPs – for brine treatment due to the impact of
468 halides on reaction order. Instead, energy cost calculations for brine treatment by plasma must account for
469 complexities arising from the non-steady-state concentrations of hypohalous acids generated during plasma
470 exposure.

471 **Acknowledgments**

472 This work is supported by the U.S. National Science Foundation (ECO-CBET 2033714) and
473 Princeton Collaborative Research Facility, which is supported by the U.S. Department of Energy (DOE)
474 under Contract No. DE-AC02-09CH11466. We thank Dr. Trey Oldham and Dr. Xiaoshuang Chen for
475 training in plasma operations, Dr. Daniel Giammar for providing some chemicals, Dr. Yinjie Tang and Dr.
476 Marcus Foston for access to the UV–vis spectrophotometer and conductivity meter, respectively, and Brent
477 Dummitt for making the custom glass vessel. We thank the Institute of Materials Science and Engineering
478 at Washington University in St. Louis for the use of material characterization facility.

479 **Conflict of Interest**

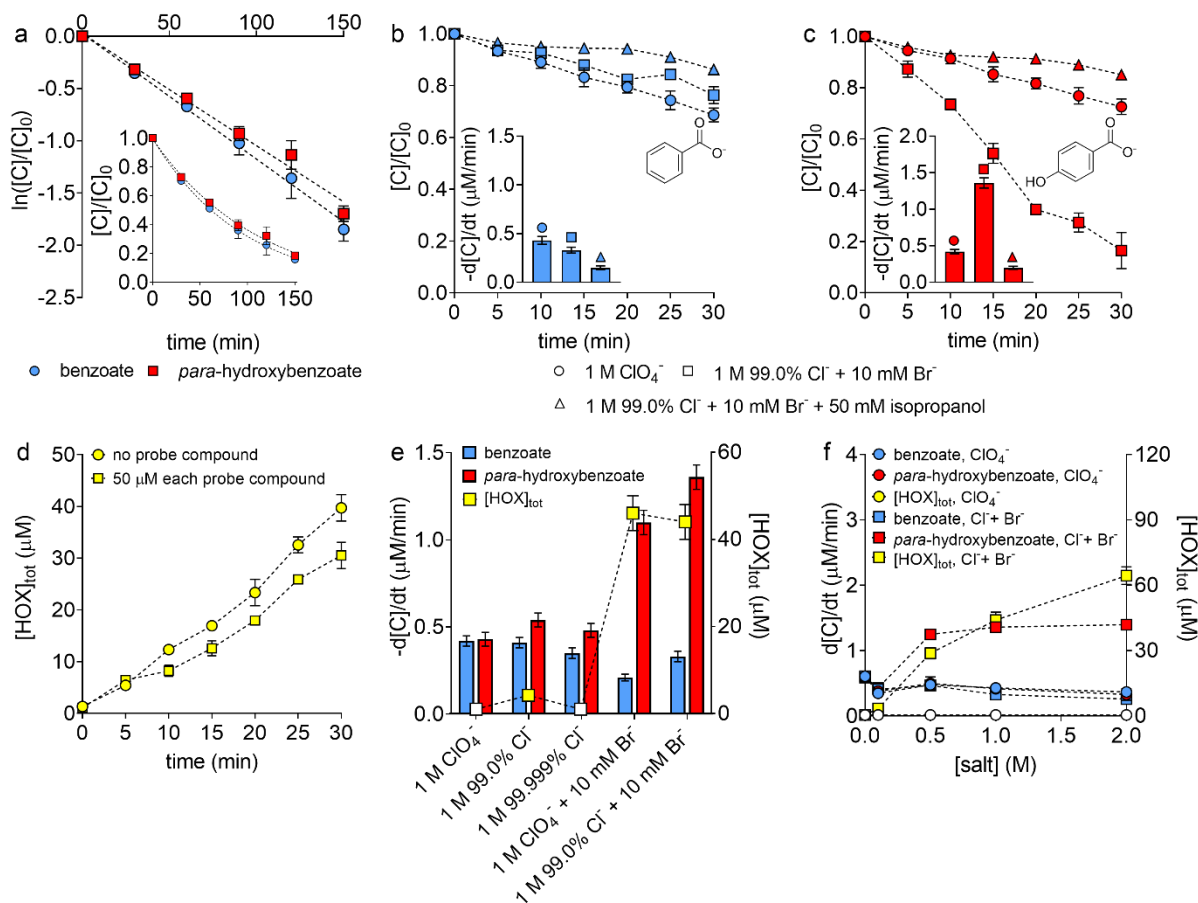
480 The authors declare no competing financial interest.

481 **Supporting Information**

482 The supporting information is available free of charge at <http://pubs.acs.org>.

483 Chemical sources, brine constituents, compound selection, analytical methods, supporting results, and data
484 analysis.

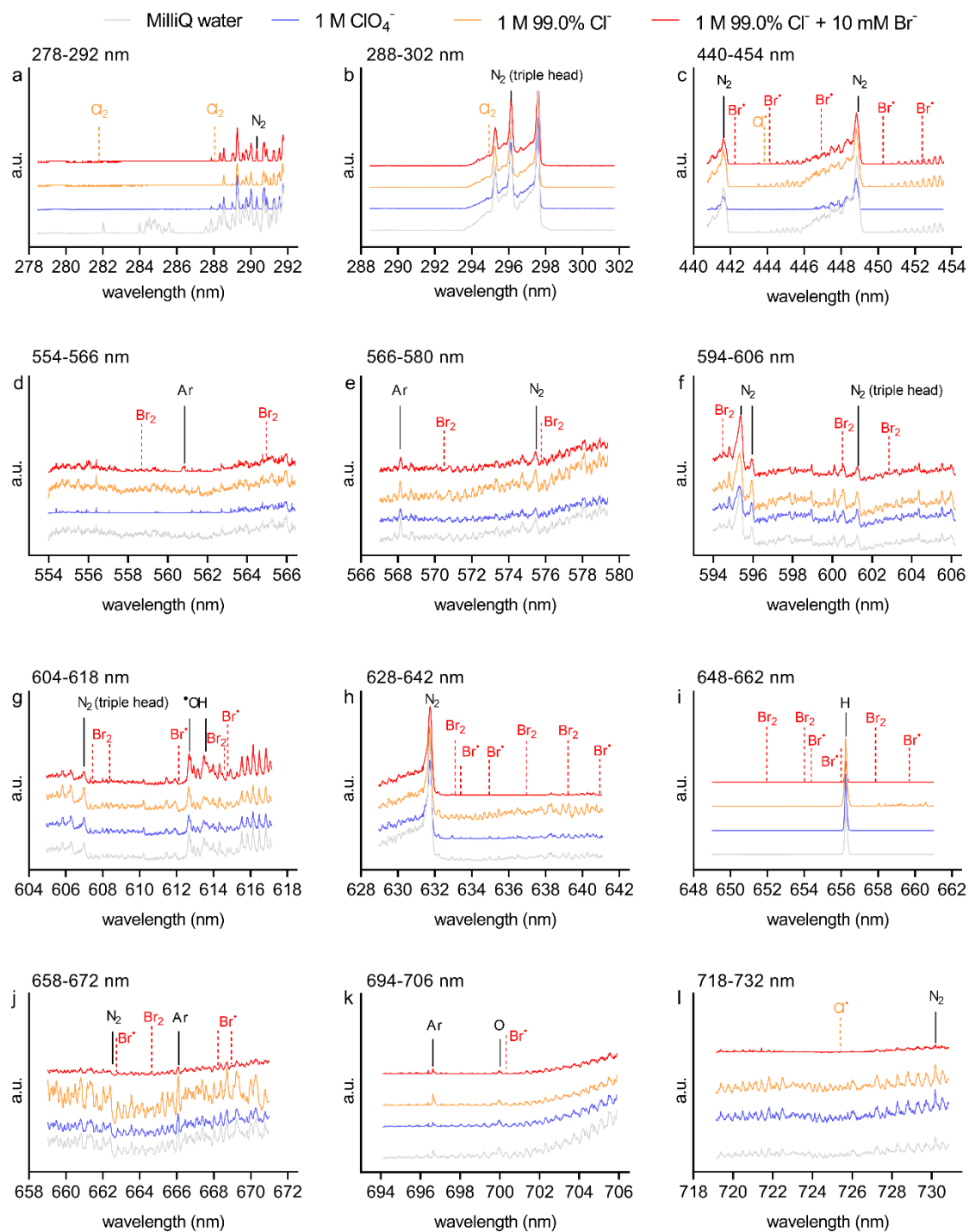
485 **Figures**



486 **Figure 1.** Degradation of probe compounds (i.e., benzoate, *para*-hydroxybenzoate) and formation of
 487 hypohalous acids during plasma treatment of solutions with varying chemical constituents (all containing
 488 10 mM phosphate buffer, pH 7). (a) Degradation of benzoate and *para*-hydroxybenzoate (each initially
 489 present at 50 μM) in the presence of 1 M ClO₄⁻. (b-c) Degradation of (b) benzoate and (c) *para*-
 490 hydroxybenzoate in the presence of salts and/or isopropanol. (d) Formation of hypohalous acids in the
 491 presence of 1 M Cl⁻ and 10 mM Br⁻. (e) Degradation rates of probe compounds and hypohalous acid
 492 concentrations (plotted on the right y-axis) in solutions with different halide combinations after plasma
 493 treatment for 30 min. For corresponding conditions, results in (e) are from the same experiments used to
 494 obtain results presented in (b-c), while results presented in (d) were collected independently to reduce the
 495 volume of solution removed during the experiments. The measured concentrations of hypohalous acids at
 496 30 min under the same condition (with probe compounds and halides) in (d) and (e) had no significant

498 difference ($p=0.10$). **(f)** Degradation rates of probe compounds and hypohalous acid concentrations (plotted
499 on the right y-axis) over 30 min in the presence of ClO_4^- or halides (i.e., Cl^- , purity: 99.0%, with 1 mol
500 percent added Br^-); results collected with 1 M salt are reproduced from **(b-c)** for probe compound
501 degradation rates and **(e)** for hypohalous acid concentration. White squares (in **e**) and circles (in **f**) represent
502 measurements below the LOD ($[\text{HOX}]_{\text{tot}} = 0.8 \mu\text{M}$). Errors on concentrations represent the range of
503 measurements from duplicate experiments, while errors on degradation rates represent the standard errors
504 of the slopes obtained from linear regression.

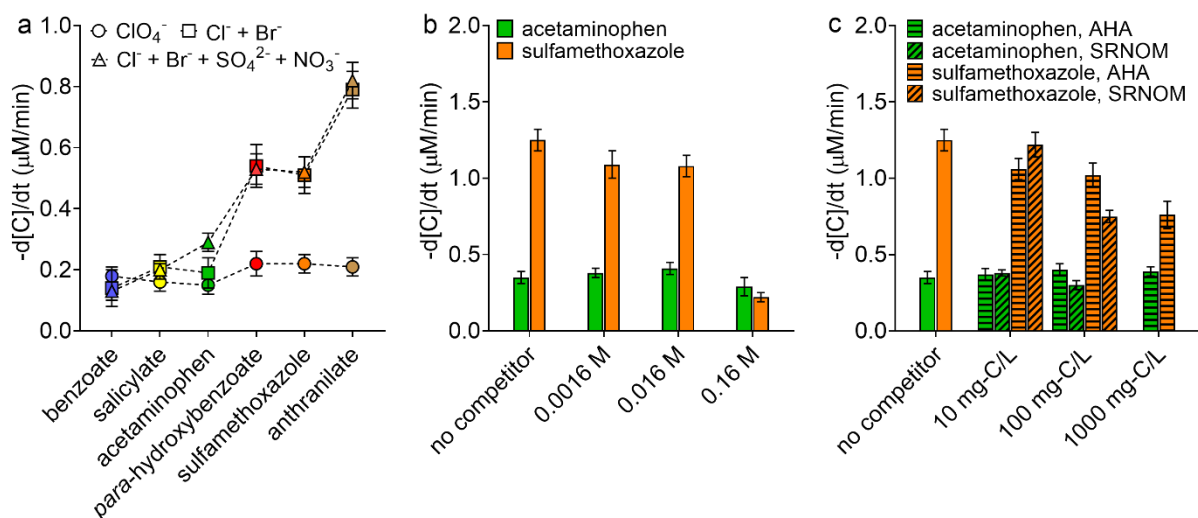
505



506
 507 **Figure 2.** High-resolution OES spectra at selected wavelengths from 278 to 732 nm in plasma over either
 508 MilliQ water or solutions containing salts. Solutions containing salts also contained 10 mM phosphate
 509 buffer (pH 7) and 50 μ M each benzoate and *para*-hydroxybenzoate. The black solid lines indicate

510 wavelengths where oxygen, nitrogen, and argon species were identified. The orange and red dashed lines
511 indicate wavelengths where halogen radicals and molecular halogens were previously reported (**Table**
512 **S7**)^{133,134} but not identified in this study.

513



514
515 **Figure 3.** Degradation rates of selected compounds during plasma treatment of solutions with additional
516 brine constituents. All solutions contained 10 mM phosphate buffer (pH 7) and had ionic strength adjusted
517 to 2.0 M by ClO_4^- . (a) Degradation rates of benzoate, salicylate, acetaminophen, *para*-hydroxybenzoate,
518 sulfamethoxazole, and anthranilate (each initially present at 50 μM) in the presence of salts. The
519 concentrations of Cl^- , Br^- , SO_4^{2-} , and NO_3^- , when present, were 1 M, 10 mM, 0.25 M, and 0.08 M,
520 respectively. (b-c) Degradation rates of acetaminophen and sulfamethoxazole (each initially present at 50
521 μM) in the presence of (b) carbonates or (c) organic matter (i.e., Aldrich humic acid, AHA; Suwannee
522 River natural organic matter, SRNOM). All solutions in (b-c) initially contained Cl^- , Br^- , SO_4^{2-} , and NO_3^-
523 at concentrations used in (a). The data in (b) and (c) for the degradation rates of acetaminophen and
524 sulfamethoxazole in the absence of competitors were obtained from the same experiments. Errors on
525 degradation rates represent the standard errors of the slopes obtained from linear regression.

526

527 **References:**

- 528 (1) Rezaei, F.; Vanraes, P.; Nikiforov, A.; Morent, R.; De Geyter, N. Applications of Plasma-Liquid
529 Systems : A Review. *Materials*. **2019**, *12* (17), 2751.
530 <https://doi.org/https://doi.org/10.3390/ma12172751>.
- 531 (2) Foster, J. E. Plasma-Based Water Purification: Challenges and Prospects for the Future. *Phys.*
532 *Plasmas* **2017**, *24* (5), 055501. <https://doi.org/10.1063/1.4977921>.
- 533 (3) Wang, X.; Zhou, M.; Jin, X. Application of Glow Discharge Plasma for Wastewater Treatment.
534 *Electrochim. Acta* **2012**, *83*, 501–512. <https://doi.org/10.1016/j.electacta.2012.06.131>.
- 535 (4) Zeghioud, H.; Nguyen-Tri, P.; Khezami, L.; Amrane, A.; Assadi, A. A. Review on Discharge
536 Plasma for Water Treatment: Mechanism, Reactor Geometries, Active Species and Combined
537 Processes. *J. Water Process Eng.* **2020**, *38*, 101664. <https://doi.org/10.1016/j.jwpe.2020.101664>.
- 538 (5) Foster, J.; Sommers, B. S.; Gucker, S. N.; Blankson, I. M.; Adamovsky, G. Perspectives on the
539 Interaction of Plasmas with Liquid Water for Water Purification. *IEEE Trans. Plasma Sci.* **2012**,
540 *40* (5), 1311–1323. <https://doi.org/10.1109/TPS.2011.2180028>.
- 541 (6) Sharma, A. K.; Josephson, G. B.; Camaioni, D. M.; Goheen, S. C. Destruction of
542 Pentachlorophenol Using Glow Discharge Plasma Process. *Environ. Sci. Technol.* **2000**, *34* (11),
543 2267–2272. <https://doi.org/10.1021/es981001i>.
- 544 (7) Stratton, G. R.; Dai, F.; Bellona, C. L.; Holsen, T. M.; Dickenson, E. R. V.; Mededovic Thagard,
545 S. Plasma-Based Water Treatment: Efficient Transformation of Perfluoroalkyl Substances in
546 Prepared Solutions and Contaminated Groundwater. *Environ. Sci. Technol.* **2017**, *51* (3), 1643–
547 1648. <https://doi.org/10.1021/acs.est.6b04215>.
- 548 (8) Bruggeman, P. J.; Kushner, M. J.; Locke, B. R.; Gardeniers, J. G. E.; Graham, W. G.; Graves, D.
549 B.; Hofman-Caris, R. C. H. M.; Maric, D.; Reid, J. P.; Ceriani, E.; Fernandez Rivas, D.; Foster, J.

550 E. Garrick, S. C.; Gorbanev, Y.; Hamaguchi, S.; Iza, F.; Jablonowski, H.; Klimova, E.;
551 Kolb, J.; Krcma, F.; Lukes, P.; MacHala, Z.; Marinov, I.; Mariotti, D.; Mededovic
552 Thagard, S.; Minakata, D.; Neyts, E. C.; Pawlat, J.; Petrovic, Z. L.; Pflieger, R.; Reuter,
553 S.; Schram, D. C.; Schröter, S.; Shiraiwa, M.; Tarabová, B.; Tsai, P. A.; Verlet, J. R.R.;
554 Von Woedtke, T.; Wilson, K. R.; Yasui, K.; Zvereva, G. Plasma-Liquid Interactions: A
555 Review and Roadmap. *Plasma Sources Sci. Technol.* **2016**, *25* (5). [https://doi.org/10.1088/0963-](https://doi.org/10.1088/0963-0252/25/5/053002)
556 [0252/25/5/053002](https://doi.org/10.1088/0963-0252/25/5/053002).

557 (9) Tachibana, K.; Nakamura, T. Comparative Study of Discharge Schemes for Production Rates and
558 Ratios of Reactive Oxygen and Nitrogen Species in Plasma Activated Water. *J. Phys. D. Appl.*
559 *Phys.* **2019**, *52* (38). <https://doi.org/10.1088/1361-6463/ab2529>.

560 (10) Zhang, X.; Zhou, R.; Bazaka, K.; Liu, Y.; Zhou, R.; Chen, G.; Chen, Z.; Liu, Q.; Yang, S.;
561 Ostrikov, K. Quantification of Plasma Produced OH Radical Density for Water Sterilization.
562 *Plasma Process. Polym.* **2018**, *15* (6). <https://doi.org/10.1002/ppap.201700241>.

563 (11) Franclemont, J.; Fan, X.; Thagard, S. M. Physicochemical Mechanisms of Plasma-Liquid
564 Interactions within Plasma Channels in Liquid. *J. Phys. D. Appl. Phys.* **2015**, *48* (42).
565 <https://doi.org/10.1088/0022-3727/48/42/424004>.

566 (12) Buxton, G. V.; Greenstock, C. L.; Helman, W. P.; Ross, A. B. Critical Review of Rate Constants
567 for Reactions of Hydrated Electrons, Hydrogen Atoms and Hydroxyl Radicals ($\cdot\text{OH}/\cdot\text{O}^-$) in
568 Aqueous Solutions. *J. Phys. Chem. Ref. Data* **1988**, *17* (2), 513–886.
569 <https://doi.org/10.1063/1.555805>.

570 (13) Wardenier, N.; Gorbanev, Y.; Van Moer, I.; Nikiforov, A.; Van Hulle, S. W. H.; Surmont, P.;
571 Lynen, F.; Leys, C.; Bogaerts, A.; Vanraes, P. Removal of Alachlor in Water by Non-Thermal
572 Plasma: Reactive Species and Pathways in Batch and Continuous Process. *Water Res.* **2019**, *161*,
573 549–559. <https://doi.org/10.1016/j.watres.2019.06.022>.

- 574 (14) Magureanu, M.; Bradu, C.; Parvulescu, V. I. Plasma Processes for the Treatment of Water
575 Contaminated with Harmful Organic Compounds. *J. Phys. D. Appl. Phys.* **2018**, *51* (31).
576 <https://doi.org/10.1088/1361-6463/aacd9c>.
- 577 (15) Sarangapani, C.; Misra, N. N.; Milosavljevic, V.; Bourke, P.; O'Regan, F.; Cullen, P. J. Pesticide
578 Degradation in Water Using Atmospheric Air Cold Plasma. *J. Water Process Eng.* **2016**, *9*, 225–
579 232. <https://doi.org/10.1016/j.jwpe.2016.01.003>.
- 580 (16) Banaschik, R.; Jablonowski, H.; Bednarski, P. J.; Kolb, J. F. Degradation and Intermediates of
581 Diclofenac as Instructive Example for Decomposition of Recalcitrant Pharmaceuticals by
582 Hydroxyl Radicals Generated with Pulsed Corona Plasma in Water. *J. Hazard. Mater.* **2018**, *342*,
583 651–660. <https://doi.org/10.1016/j.jhazmat.2017.08.058>.
- 584 (17) Magureanu, M.; Piroi, D.; Mandache, N. B.; David, V.; Medvedovici, A.; Bradu, C.; Parvulescu,
585 V. I. Degradation of Antibiotics in Water by Non-Thermal Plasma Treatment. *Water Res.* **2011**, *45*
586 (11), 3407–3416. <https://doi.org/10.1016/j.watres.2011.03.057>.
- 587 (18) Wang, R.; Wang, T.; Qu, G.; Zhang, Y.; Guo, X.; Jia, H.; Zhu, L. Insights into the Underlying
588 Mechanisms for Integrated Inactivation of *A. Spiroides* and Depression of Disinfection
589 Byproducts by Plasma Oxidation. *Water Res.* **2021**, *196*, 117027.
590 <https://doi.org/10.1016/j.watres.2021.117027>.
- 591 (19) Xin, Q.; Zhang, Y.; Wu, K. Degradation of Microcystin-LR by Gas-Liquid Interfacial Discharge
592 Plasma. *Plasma Sci. Technol.* **2013**, *15* (12), 1221–1225. [https://doi.org/10.1088/1009-](https://doi.org/10.1088/1009-0630/15/12/11)
593 [0630/15/12/11](https://doi.org/10.1088/1009-0630/15/12/11).
- 594 (20) Zhang, H.; Huang, Q.; Ke, Z.; Yang, L.; Wang, X.; Yu, Z. Degradation of Microcystin-LR in
595 Water by Glow Discharge Plasma Oxidation at the Gas-Solution Interface and Its Safety
596 Evaluation. *Water Res.* **2012**, *46* (19), 6554–6562. <https://doi.org/10.1016/j.watres.2012.09.041>.

- 597 (21) Rumbach, P.; Bartels, D. M.; Sankaran, R. M.; Go, D. B. The Solvation of Electrons by an
598 Atmospheric-Pressure Plasma. *Nat. Commun.* **2015**, *6*. <https://doi.org/10.1038/ncomms8248>.
- 599 (22) Richmonds, C.; Witzke, M.; Bartling, B.; Lee, S. W.; Wainright, J.; Liu, C.; Sankaran, R. M.
600 Electron-Transfer Reactions at the Plasma À Liquid Interface. *J. Am. Chem. Soc.* **2011**, *133*,
601 17582–17585. <https://doi.org/10.1021/ja207547b>
- 602 (23) Ilich, P. P.; McCormick, K. R.; Atkins, A. D.; Mell, G. J.; Flaherty, T. J.; Bruck, M. J.; Goodrich,
603 H. A.; Hefel, A. L.; Juranić, N.; Seleem, S. Solvated Electrons in Organic Chemistry Laboratory.
604 *J. Chem. Educ.* **2010**, *87* (4), 419–422. <https://doi.org/10.1021/ed800093n>.
- 605 (24) Abel, B.; Buck, U.; Sobolewski, A. L.; Domcke, W. On the Nature and Signatures of the Solvated
606 Electron in Water. *Phys. Chem. Chem. Phys.* **2012**, *14* (1), 22–34.
607 <https://doi.org/10.1039/c1cp21803d>.
- 608 (25) Neta, P. Reactions of Hydrogen Atoms in Aqueous Solutions. *Chem. Rev.* **1972**, *75* (5), 533–543.
609 <https://doi.org/https://doi.org/10.1021/cr60279a005>.
- 610 (26) Mededovic Thagard, S.; Stratton, G. R.; Dai, F.; Bellona, C. L.; Holsen, T. M.; Bohl, D. G.; Paek,
611 E.; Dickenson, E. R. V. Plasma-Based Water Treatment: Development of a General Mechanistic
612 Model to Estimate the Treatability of Different Types of Contaminants. *J. Phys. D. Appl. Phys.*
613 **2017**, *50* (1). <https://doi.org/10.1088/1361-6463/50/1/014003>.
- 614 (27) Gao, X.; Wang, X.; Ma, J.; Liu, Y. Potential and Mechanism of Disinfection By-products
615 Removal in Drinking Water by Bubbling Corona Discharge. *Water Res.* **2023**, *245*, 120624.
616 <https://doi.org/10.1016/j.watres.2023.120624>.
- 617 (28) Zhao, Y.; Zhang, C.; Chu, L.; Zhou, Q.; Huang, B. Hydrated Electron Based Photochemical
618 Processes for Water Treatment. *Water Res.* **2022**, *225*, 119212.
619 <https://doi.org/10.1016/j.watres.2022.119212>.

- 620 (29) Bentel, M. J.; Yu, Y.; Xu, L.; Li, Z.; Wong, B. M.; Men, Y.; Liu, J. Defluorination of Per- and
621 Polyfluoroalkyl Substances (PFASs) with Hydrated Electrons: Structural Dependence and
622 Implications to PFAS Remediation and Management. *Environ. Sci. Technol.* **2019**, *53* (7), 3718–
623 3728. <https://doi.org/10.1021/acs.est.8b06648>.
- 624 (30) Singh, R. K.; Multari, N.; Nau-Hix, C.; Anderson, R. H.; Richardson, S. D.; Holsen, T. M.;
625 Mededovic Thagard, S. Rapid Removal of Poly- and Perfluorinated Compounds from
626 Investigation-Derived Waste (IDW) in a Pilot-Scale Plasma Reactor. *Environ. Sci. Technol.* **2019**.
627 <https://doi.org/10.1021/acs.est.9b02964>.
- 628 (31) Li, X.; Fang, J.; Liu, G.; Zhang, S.; Pan, B.; Ma, J. Kinetics and Efficiency of the Hydrated
629 Electron-Induced Dehalogenation by the Sulfite/UV Process. *Water Res.* **2014**, *62* (2), 220–228.
630 <https://doi.org/10.1016/j.watres.2014.05.051>.
- 631 (32) Wu, Z.; Shang, C.; Wang, D.; Zheng, S.; Wang, Y.; Fang, J. Rapid Degradation of
632 Dichloroacetonitrile by Hydrated Electron (e_{aq}^-) Produced in Vacuum Ultraviolet Photolysis.
633 *Chemosphere* **2020**, *256*, 126994. <https://doi.org/10.1016/j.chemosphere.2020.126994>.
- 634 (33) Cole, S. K.; Cooper, W. J.; Fox, R. V.; Gardinali, P. R.; Mezyk, S. P.; Mincher, B. J.; O'Shea, K.
635 E. Free Radical Chemistry of Disinfection Byproducts. 2. Rate Constants and Degradation
636 Mechanisms of Trichloronitromethane (Chloropicrin). *Environ. Sci. Technol.* **2007**, *41* (3), 863–
637 869. <https://doi.org/10.1021/es061410b>.
- 638 (34) Liu, Z.; Haddad, M.; Sauv e, S.; Barbeau, B. Alleviating the Burden of Ion Exchange Brine in
639 Water Treatment: From Operational Strategies to Brine Management. *Water Res.* **2021**, *205*,
640 117728. <https://doi.org/10.1016/j.watres.2021.117728>.
- 641 (35) Singh, R. K.; Multari, N.; Nau-Hix, C.; Woodard, S.; Nickelsen, M.; Mededovic Thagard, S.;
642 Holsen, T. M. Removal of Poly- And Per-Fluorinated Compounds from Ion Exchange Regenerant
643 Still Bottom Samples in a Plasma Reactor. *Environ. Sci. Technol.* **2020**, *54* (21), 13973–13980.

- 644 <https://doi.org/10.1021/acs.est.0c02158>.
- 645 (36) Giwa, A.; Dufour, V.; Al Marzooqi, F.; Al Kaabi, M.; Hasan, S. W. Brine Management Methods:
646 Recent Innovations and Current Status. *Desalination* **2017**, *407*, 1–23.
647 <https://doi.org/10.1016/j.desal.2016.12.008>.
- 648 (37) Tow, E. W.; Ersan, M. S.; Kum, S.; Lee, T.; Speth, T. F.; Owen, C.; Bellona, C.; Nadagouda, M.
649 N.; Mikelonis, A. M.; Westerhoff, P.; Myrose, C.; Frenkel V.S.; deSilva, V.; Walker, W.S.;
650 Safulko, A.K.; Ladner, D.A. Managing and Treating Per- and Polyfluoroalkyl Substances (PFAS)
651 in Membrane Concentrates. *AWWA Water Sci.* **2021**, *3* (5), 1–23.
652 <https://doi.org/10.1002/aws2.1233>.
- 653 (38) Azerrad, S. P.; Lütke Eversloh, C.; Gilboa, M.; Schulz, M.; Ternes, T.; Dosoretz, C. G.
654 Identification of Transformation Products during Advanced Oxidation of Diatrizoate: Effect of
655 Water Matrix and Oxidation Process. *Water Res.* **2016**, *103*, 424–434.
656 <https://doi.org/10.1016/j.watres.2016.07.066>.
- 657 (39) Jose, J.; Philip, L. Continuous Flow Pulsed Power Plasma Reactor for the Treatment of Aqueous
658 Solution Containing Volatile Organic Compounds and Real Pharmaceutical Wastewater. *J.*
659 *Environ. Manage.* **2021**, *286*, 112202. <https://doi.org/10.1016/j.jenvman.2021.112202>.
- 660 (40) Manakhov, A.; Orlov, M.; Grokhovsky, V.; Alghunaimi, F. I.; Ayirala, S. Functionalized
661 Nanomembranes and Plasma Technologies for Produced Water Treatment a Review. *Polymers.*
662 **2022**, *14* (9). <https://doi.org/10.3390/polym14091785>.
- 663 (41) Sun, M.; Lowry, G. V.; Gregory, K. B. Selective Oxidation of Bromide in Wastewater Brines from
664 Hydraulic Fracturing. *Water Res.* **2013**, *47* (11), 3723–3731.
665 <https://doi.org/10.1016/j.watres.2013.04.041>.
- 666 (42) Singh, R. K.; Brown, E.; Mededovic Thagard, S.; Holsen, T. M. Treatment of PFAS-Containing

- 667 Landfill Leachate Using an Enhanced Contact Plasma Reactor. *J. Hazard. Mater.* **2021**, *408*,
668 124452. <https://doi.org/10.1016/j.jhazmat.2020.124452>.
- 669 (43) Sathiyaraj, G.; Chellappan Ravindran, K.; Hussain Malik, Z. Physico-Chemical Characteristics of
670 Textile Effluent Collected from Erode, Pallipalayam and Bhavani Polluted Regions, Tamilnadu,
671 India. *J. Ecobiotechnology* **2017**, *9*, 1–4. <https://doi.org/10.19071/jebt.2017.v9.3191>.
- 672 (44) Rodriguez, E. E.; Tarpeh, W. A.; Wigginton, K. R.; Love, N. G. Application of Plasma for the
673 Removal of Pharmaceuticals in Synthetic Urine. *Environ. Sci. Water Res. Technol.* **2022**, *8* (3),
674 523–533. <https://doi.org/10.1039/d1ew00863c>.
- 675 (45) Nau-Hix, C.; Holsen, T. M.; Thagard, S. M. Influence of Solution Electrical Conductivity and
676 Ionic Composition on the Performance of a Gas-Liquid Pulsed Spark Discharge Reactor for Water
677 Treatment. *J. Appl. Phys.* **2021**, *130* (12), 123301. <https://doi.org/10.1063/5.0054327>.
- 678 (46) Li, Z.; Lyu, X.; Gao, B.; Xu, H.; Wu, J.; Sun, Y. Effects of Ionic Strength and Cation Type on the
679 Transport of Perfluorooctanoic Acid (PFOA) in Unsaturated Sand Porous Media. *J. Hazard.*
680 *Mater.* **2021**, *403*, 123688. <https://doi.org/10.1016/j.jhazmat.2020.123688>.
- 681 (47) Lyu, Y.; Brusseau, M. L. The Influence of Solution Chemistry on Air-Water Interfacial
682 Adsorption and Transport of PFOA in Unsaturated Porous Media. *Sci. Total Environ.* **2020**, *713*,
683 136744. <https://doi.org/10.1016/j.scitotenv.2020.136744>.
- 684 (48) Le, S. T.; Gao, Y.; Kibbey, T. C. G.; Glamore, W. C.; O'Carroll, D. M. Predicting the Impact of
685 Salt Mixtures on the Air-Water Interfacial Behavior of PFAS. *Sci. Total Environ.* **2022**, *819*,
686 151987. <https://doi.org/10.1016/j.scitotenv.2021.151987>.
- 687 (49) Shih, K. Y.; Locke, B. R. Optical and Electrical Diagnostics of the Effects of Conductivity on
688 Liquid Phase Electrical Discharge. *IEEE Trans. Plasma Sci.* **2011**, *39* (3), 883–892.
689 <https://doi.org/10.1109/TPS.2010.2098052>.

- 690 (50) Thagard, S. M.; Takashima, K.; Mizuno, A. Chemistry of the Positive and Negative Electrical
691 Discharges Formed in Liquid Water and above a Gas-Liquid Surface. *Plasma Chem. Plasma*
692 *Process.* **2009**, *29* (6), 455–473. <https://doi.org/10.1007/s11090-009-9195-x>.
- 693 (51) El-Tayeb, A.; El-Shazly, A. H.; Elkady, M. F. Investigation the Influence of Different Salts on the
694 Degradation of Organic Dyes Using Non-Thermal Plasma. *Energies* **2016**, *9* (11), 874.
695 <https://doi.org/10.3390/en9110874>.
- 696 (52) Zhu, D.; Sun, Z.; Zhang, H.; Zhang, A.; Zhang, Y.; Miruka, A. C.; Zhu, L.; Li, R.; Guo, Y.; Liu,
697 Y. Reactive Nitrogen Species Generated by Gas–Liquid Dielectric Barrier Discharge for Efficient
698 Degradation of Perfluorooctanoic Acid from Water. *Environ. Sci. Technol.* **2022**, *56* (1), 349–360.
699 <https://doi.org/10.1021/acs.est.1c06342>.
- 700 (53) Yi, R.; Yi, C.; Du, D.; Zhang, Q.; Yu, H.; Yang, L. Research on Quinoline Degradation in
701 Drinking Water by a Large Volume Strong Ionization Dielectric Barrier Discharge Reaction
702 System. *Plasma Sci. Technol.* **2021**, *23* (8), 085505.
- 703 (54) Haghghat, G.; Sohrabi, A.; Shaibani, P. M.; Van Neste, C. W.; Naicker, S.; Thundat, T. The Role
704 of Chloride Ions in Plasma-Activated Water Treatment Processes. *Environ. Sci. Water Res.*
705 *Technol.* **2017**, *3* (1), 156–168. <https://doi.org/10.1039/c6ew00308g>.
- 706 (55) Wang, L. Aqueous Organic Dye Discoloration Induced by Contact Glow Discharge Electrolysis.
707 *J. Hazard. Mater.* **2009**, *171* (1–3), 577–581. <https://doi.org/10.1016/j.jhazmat.2009.06.037>.
- 708 (56) Wang, L.; Jiang, X.; Liu, Y. Degradation of Bisphenol A and Formation of Hydrogen Peroxide
709 Induced by Glow Discharge Plasma in Aqueous Solutions. *J. Hazard. Mater.* **2008**, *154* (1–3),
710 1106–1114. <https://doi.org/10.1016/j.jhazmat.2007.11.016>.
- 711 (57) Jirásek, V.; Lukeš, P. Formation of Reactive Chlorine Species in Saline Solution Treated by Non-
712 Equilibrium Atmospheric Pressure He/O₂ Plasma Jet. *Plasma Sources Sci. Technol.* **2019**, *28* (3).

- 713 <https://doi.org/10.1088/1361-6595/ab0930>.
- 714 (58) Jirásek, V.; Lukeš, P. Competitive Reactions in Cl^- Solutions Treated by Plasma-Supplied O
715 Atoms. *J. Phys. D. Appl. Phys.* **2020**, *53*, 505206. <https://doi.org/10.1088/1361-6463/abb5d6>.
- 716 (59) Gorbanev, Y.; Van Der Paal, J.; Van Boxem, W.; Dewilde, S.; Bogaerts, A. Reaction of Chloride
717 Anion with Atomic Oxygen in Aqueous Solutions: Can Cold Plasma Help in Chemistry Research?
718 *Phys. Chem. Chem. Phys.* **2019**, *21* (8), 4117–4121. <https://doi.org/10.1039/c8cp07550f>.
- 719 (60) Wu, D.; Wong, D.; Di Bartolo, B. Evolution of Cl_2^- in Aqueous NaCl Solutions. *J. Photochem.*
720 **1980**, *14* (4), 303–310. [https://doi.org/10.1016/0047-2670\(80\)85102-1](https://doi.org/10.1016/0047-2670(80)85102-1).
- 721 (61) Yu, X. Y.; Bao, Z. C.; Barker, J. R. Free Radical Reactions Involving Cl^\cdot , Cl_2^\cdot , and SO_4^\cdot in the
722 248 nm Photolysis of Aqueous Solutions Containing $\text{S}_2\text{O}_8^{2-}$ and Cl^- . *J. Phys. Chem. A* **2004**, *108*
723 (2), 295–308. <https://doi.org/10.1021/jp036211i>.
- 724 (62) Deborde, M.; von Gunten, U. Reactions of Chlorine with Inorganic and Organic Compounds
725 during Water Treatment-Kinetics and Mechanisms: A Critical Review. *Water Res.* **2008**, *42* (1–2),
726 13–51. <https://doi.org/10.1016/j.watres.2007.07.025>.
- 727 (63) Magazinovic, R. S.; Nicholson, B. C.; Mulcahy, D. E.; Davey, D. E. Bromide Levels in Natural
728 Waters: Its Relationship to Levels of Both Chloride and Total Dissolved Solids and the
729 Implications for Water Treatment. *Chemosphere* **2004**, *57* (4), 329–335.
730 <https://doi.org/10.1016/j.chemosphere.2004.04.056>.
- 731 (64) Yang, Y.; Pignatello, J. J.; Ma, J.; Mitch, W. A. Effect of Matrix Components on UV/ H_2O_2 and
732 UV/ $\text{S}_2\text{O}_8^{2-}$ Advanced Oxidation Processes for Trace Organic Degradation in Reverse Osmosis
733 Brines from Municipal Wastewater Reuse Facilities. *Water Res.* **2016**, *89*, 192–200.
734 <https://doi.org/10.1016/j.watres.2015.11.049>.
- 735 (65) Justo, A.; González, O.; Aceña, J.; Pérez, S.; Barceló, D.; Sans, C.; Esplugas, S. Pharmaceuticals

- 736 and Organic Pollution Mitigation in Reclamation Osmosis Brines by UV/H₂O₂ and Ozone. *J.*
737 *Hazard. Mater.* **2013**, *263*, 268–274. <https://doi.org/10.1016/j.jhazmat.2013.05.030>.
- 738 (66) Zhang, K.; Parker, K. M.. Halogen Radical Oxidants in Natural and Engineered Aquatic Systems.
739 *Environ. Sci. Technol.* **2018**, *52* (17), 9579–9594. <https://doi.org/10.1021/acs.est.8b02219>.
- 740 (67) Grebel, J. E.; Pignatello, J. J.; Mitch, W. A. Effect of Halide Ions and Carbonates on Organic
741 Contaminant Degradation by Hydroxyl Radical-Based Advanced Oxidation Processes in Saline
742 Waters. *Environ. Sci. Technol.* **2010**, *44* (17), 6822–6828. <https://doi.org/10.1021/es1010225>.
- 743 (68) Yang, Y.; Pignatello, J. J.; Ma, J.; Mitch, W. A. Comparison of Halide Impacts on the Efficiency
744 of Contaminant Degradation by Sulfate and Hydroxyl Radical-Based Advanced Oxidation
745 Processes (AOPs). *Environ. Sci. Technol.* **2014**. <https://doi.org/10.1021/es404118q>.
- 746 (69) Jayson, G. G.; Parsons, B. J.; Swallow, A. J. Some Simple, Highly Reactive, Inorganic Chlorine
747 Derivatives in Aqueous Solution. Their Formation Using Pulses of Radiation and Their Role in the
748 Mechanism of the Fricke Dosimeter. *J. Chem. Soc. Faraday Trans* **1973**, *69* (9), 1597–1607.
- 749 (70) Klänig, U. K.; Wolff, T. Laser Flash Photolysis of HClO, ClO⁻, HBrO, and BrO⁻ in Aqueous
750 Solution. Reactions of Cl⁻ and Br⁻ Atoms. *Berichte der Bunsengesellschaft für Phys. Chemie* **1985**,
751 *89* (3), 243–245.
- 752 (71) Grigorev, A. E.; Makarov, I. E.; Pikaev, A. K. Formation of Cl₂⁻ in the Bulk Solution during the
753 Radiolysis of Concentrated Aqueous Solution of Chlorides. *High Energy Chem.* **1987**, *21*, 99–102.
- 754 (72) Zehavi, D.; Rabani, J. The Oxidation of Aqueous Bromide Ions by Hydroxyl Radicals. A Pulse
755 Radiolytic Investigation. *J. Phys. Chem.* **1972**, *76* (3), 312–319.
756 <https://doi.org/10.1021/j100647a006>.
- 757 (73) Merényi, G.; Lind, J. Reaction Mechanism of Hydrogen Abstraction by the Bromine Atom in
758 Water. *J. Am. Chem. Soc.* **1994**, *116* (17), 7872–7876. <https://doi.org/10.1021/ja00096a050>.

- 759 (74) Matthew, B. M.; Anastasio, C. A Chemical Probe Technique for the Determination of Reactive
760 Halogen Species in Aqueous Solution: Part 1 - Bromide Solutions. *Atmos. Chem. Phys.* **2006**, *6*
761 (9), 2423–2437 <https://doi.org/10.5194/acp-6-2423-2006>.
- 762 (75) Westerhoff, P.; Chao, P.; Mash, H. Reactivity of Natural Organic Matter with Aqueous Chlorine
763 and Bromine. *Water Res.* **2004**, *38* (6), 1502–1513. <https://doi.org/10.1016/j.watres.2003.12.014>.
- 764 (76) Ershov, B. G. Kinetics, Mechanism and Intermediates of Some Radiation-Induced Reactions in
765 Aqueous Solutions. *Usp. Khim.* **2004**, *73* (1), 107–120.
766 <https://doi.org/10.1070/rc2004v073n01abeh000865>.
- 767 (77) Heeb, M. B.; Criquet, J.; Zimmermann-Steffens, S. G.; Von Gunten, U. Oxidative Treatment of
768 Bromide-Containing Waters: Formation of Bromine and Its Reactions with Inorganic and Organic
769 Compounds - A Critical Review. *Water Res.* **2014**, *48* (1), 15–42.
770 <https://doi.org/10.1016/j.watres.2013.08.030>.
- 771 (78) Wagner, I.; Karthaeuser, J.; Strehlow, H. On the Decay of the Dichloride Anion Cl₂⁻ in Aqueous
772 Solution. *Berichte der Bunsengesellschaft für Phys. Chemie* **1986**, *90* (10), 861–867.
773 <https://doi.org/https://doi.org/10.1002/bbpc.19860901007>.
- 774 (79) Wagner, I.; Strehlow, H. On the Flash Photolysis of Bromide Ions in Aqueous Solutions. *Berichte*
775 *der Bunsengesellschaft für Phys. Chemie* **1987**, *91* (12), 1317–1321.
776 <https://doi.org/https://doi.org/10.1002/bbpc.19870911203>.
- 777 (80) Wong, D.; Di Bartolo, B. Evolution of the Dihalide Ion Br₂⁻ in Aqueous Solutions. *J. Photochem.*
778 **1975**, *4* (4), 249–268. [https://doi.org/10.1016/0047-2670\(75\)87003-1](https://doi.org/10.1016/0047-2670(75)87003-1).
- 779 (81) Feng, Y.; Smith, D. W.; Bolton, J. R. Photolysis of Aqueous Free Chlorine Species (HOCl and
780 OCl⁻) with 254 nm Ultraviolet Light. *J. Environ. Eng. Sci.* **2007**, *6* (3), 277–284.
781 <https://doi.org/10.1139/s06-052>.

- 782 (82) Zeng, T.; Wilson, C. J.; Mitch, W. A. Effect of Chemical Oxidation on the Sorption Tendency of
783 Dissolved Organic Matter to a Model Hydrophobic Surface. *Environ. Sci. Technol.* **2014**, *48* (9),
784 5118–5126. <https://doi.org/10.1021/es405257b>.
- 785 (83) Moravej, M.; Yang, X.; Nowling, G. R.; Chang, J. P.; Hicks, R. F.; Babayan, S. E. Physics of
786 High-Pressure Helium and Argon Radio-Frequency Plasmas. *J. Appl. Phys.* **2004**, *96* (12), 7011–
787 7017. <https://doi.org/10.1063/1.1815047>.
- 788 (84) Sun, B.; Sato, M.; Clements, J. S. Optical Study of Active Species Produced by a Pulsed Streamer
789 Corona Discharge in Water. *J. Electrostat.* **1997**, *39* (3), 189–202. <https://doi.org/10.1016/S0304->
790 3886(97)00002-8.
- 791 (85) Rumbach, P.; Bartels, D. M.; Sankaran, R. M.; Go, D. B. The Effect of Air on Solvated Electron
792 Chemistry at a Plasma/Liquid Interface. *J. Phys. D. Appl. Phys.* **2015**, *48* (42), 424001.
793 <https://doi.org/10.1088/0022-3727/48/42/424001>.
- 794 (86) Clifford, D.; Liu, X. Biological Denitrification of Spent Regenerant Brine Using a Sequencing
795 Batch Reactor. *Water Res.* **1993**, *27* (9), 1477–1484. [https://doi.org/10.1016/0043-1354\(93\)90028-](https://doi.org/10.1016/0043-1354(93)90028-)
796 G.
- 797 (87) Haddad, M.; Bazinet, L.; Barbeau, B. Eco-Efficient Treatment of Ion Exchange Spent Brine via
798 Electrodialysis to Recover NaCl and Minimize Waste Disposal. *Sci. Total Environ.* **2019**, *690*,
799 400–409. <https://doi.org/10.1016/j.scitotenv.2019.06.539>.
- 800 (88) Haddad, M.; Bazinet, L.; Barbeau, B. Towards Water, Sodium Chloride and Natural Organic
801 Matter Recovery from Ion Exchange Spent Brine. *Membranes (Basel)*. **2021**, *11* (4), 1–13.
802 <https://doi.org/10.3390/membranes11040262>.
- 803 (89) Hiremath, T.; Roberts, D. J.; Lin, X.; Clifford, D. A.; Gillogly, T. E. T.; Lehman, S. G. Biological
804 Treatment of Perchlorate in Spent ISEP Ion-Exchange Brine. *Environ. Eng. Sci.* **2006**, *23* (6),

- 805 1009–1016. <https://doi.org/10.1089/ees.2006.23.1009>.
- 806 (90) Homan, N. P.; Green, P. G.; Young, T. M. Evaluating Ferrous Chloride for Removal of Chromium
807 From Ion-Exchange Waste Brines. *J. Am. Water Works Assoc.* **2018**, *110* (4), E43–E54.
808 <https://doi.org/10.5942/jawwa.2018.110.0022>.
- 809 (91) Hutchison, J. M.; Zilles, J. L. Biocatalytic Removal of Perchlorate and Nitrate in Ion-Exchange
810 Waste Brine. *Environ. Sci. Water Res. Technol.* **2018**, *4* (8), 1181–1189.
811 <https://doi.org/10.1039/c8ew00178b>.
- 812 (92) Korak, J. A.; Huggins, R. G.; Arias-Paić, M. S. Nanofiltration to Improve Process Efficiency of
813 Hexavalent Chromium Treatment Using Ion Exchange. *J. Am. Water Works Assoc.* **2018**, *110* (6),
814 E13–E26. <https://doi.org/10.1002/awwa.1051>.
- 815 (93) Leong, J.; Tan, J.; Heitz, A.; Ladewig, B. P. Performance of a Vibratory Shear Membrane
816 Filtration System during the Treatment of Magnetic Ion Exchange Process Concentrate.
817 *Desalination* **2015**, *365*, 196–203. <https://doi.org/10.1016/j.desal.2015.02.042>.
- 818 (94) Liu, J.; Choe, J. K.; Sasnow, Z.; Werth, C. J.; Strathmann, T. J. Application of a Re-Pd Bimetallic
819 Catalyst for Treatment of Perchlorate in Waste Ion-Exchange Regenerant Brine. *Water Res.* **2013**,
820 *47* (1), 91–101. <https://doi.org/10.1016/j.watres.2012.09.031>.
- 821 (95) McAdam, E. J.; Judd, S. J. Biological Treatment of Ion-Exchange Brine Regenerant for Re-Use: A
822 Review. *Sep. Purif. Technol.* **2008**, *62* (2), 264–272. <https://doi.org/10.1016/j.seppur.2008.01.007>.
- 823 (96) Pakzadeh, B.; Batista, J. R. Chromium Removal from Ion-Exchange Waste Brines with Calcium
824 Polysulfide. *Water Res.* **2011**, *45* (10), 3055–3064. <https://doi.org/10.1016/j.watres.2011.03.006>.
- 825 (97) Plummer, S.; Gorman, C.; Henrie, T.; Shimabuku, K.; Thompson, R.; Seidel, C. Optimization of
826 Strong-Base Anion Exchange OandM Costs for Hexavalent Chromium Treatment. *Water Res.*
827 **2018**, *139*, 420–433. <https://doi.org/10.1016/j.watres.2018.04.011>.

- 828 (98) Schaefer, C. E.; Tran, D.; Fang, Y.; Choi, Y. J.; Higgins, C. P.; Strathmann, T. J. Electrochemical
829 Treatment of Poly- and Perfluoroalkyl Substances in Brines. *Environ. Sci. Water Res. Technol.*
830 **2020**, *6* (10), 2704–2712. <https://doi.org/10.1039/d0ew00377h>.
- 831 (99) Vaudevire, E.; Radmanesh, F.; Kolkman, A.; Vughs, D.; Cornelissen, E.; Post, J.; van der Meer,
832 W. Fate and Removal of Trace Pollutants from an Anion Exchange Spent Brine during the
833 Recovery Process of Natural Organic Matter and Salts. *Water Res.* **2019**, *154*, 34–44.
834 <https://doi.org/10.1016/j.watres.2019.01.042>.
- 835 (100) Yang, T.; Doudrick, K.; Westerhoff, P. Photocatalytic Reduction of Nitrate Using Titanium
836 Dioxide for Regeneration of Ion Exchange Brine. *Water Res.* **2013**, *47* (3), 1299–1307.
837 <https://doi.org/10.1016/j.watres.2012.11.047>.
- 838 (101) Hajbi, F.; Hammi, H.; M’Nif, A. Reuse of RO Desalination Plant Reject Brine. *J. Phase Equilibria*
839 *Diffus.* **2010**, *31* (4), 341–347. <https://doi.org/10.1007/s11669-010-9727-3>.
- 840 (102) Ji, X.; Curcio, E.; Al Obaidani, S.; Di Profio, G.; Fontananova, E.; Drioli, E. Membrane
841 Distillation-Crystallization of Seawater Reverse Osmosis Brines. *Sep. Purif. Technol.* **2010**, *71* (1),
842 76–82. <https://doi.org/10.1016/j.seppur.2009.11.004>.
- 843 (103) Lior, N.; Kim, D. Quantitative Sustainability Analysis of Water Desalination – A Didactic
844 Example for Reverse Osmosis. *Desalination* **2018**, *431*, 157–170.
845 <https://doi.org/10.1016/j.desal.2017.12.061>.
- 846 (104) Opong, R. W.; Nsiah-Baafi, E.; Andrews, A.; Koomson, B. Preliminary Study on the Use of
847 Reverse Osmosis Brine and Mine Tailings as Cement Paste Mixtures for Mine Backfilling
848 Application. *Water. Air. Soil Pollut.* **2022**, *233* (12), 1–15. [https://doi.org/10.1007/s11270-022-](https://doi.org/10.1007/s11270-022-05959-1)
849 [05959-1](https://doi.org/10.1007/s11270-022-05959-1).
- 850 (105) Walker, W. S.; Kim, Y.; Lawler, D. F. Treatment of Model Inland Brackish Groundwater Reverse

851 Osmosis Concentrate with Electrodialysis - Part II: Sensitivity to Voltage Application and
852 Membranes. *Desalination* **2014**, *345*, 128–135. <https://doi.org/10.1016/j.desal.2014.04.026>.

853 (106) Eeso, K. Non-Thermal Plasma Degradation of Per- and Polyfluoroalkyl Substances from Landfill
854 Leachate. Ph.D. Dissertation, The Florida State University, Tallahassee, FL, **2022**.
855 <https://diginole.lib.fsu.edu/islandora/object/fsu:802711/datastream/PDF/view> (accessed 2023-08-
856 28).

857 (107) Ma, X.; Li, M.; Feng, C.; He, Z. Electrochemical Nitrate Removal with Simultaneous Magnesium
858 Recovery from a Mimicked RO Brine Assisted by in Situ Chloride Ions. *J. Hazard. Mater.* **2020**,
859 *388*, 122085. <https://doi.org/10.1016/j.jhazmat.2020.122085>.

860 (108) An, B.; Steinwinder, T. R.; Zhao, D. Selective Removal of Arsenate from Drinking Water Using a
861 Polymeric Ligand Exchanger. *Water Res.* **2005**, *39* (20), 4993–5004.
862 <https://doi.org/10.1016/j.watres.2005.10.014>.

863 (109) An, B.; Liang, Q.; Zhao, D. Removal of Arsenic(V) from Spent Ion Exchange Brine Using a New
864 Class of Starch-Bridged Magnetite Nanoparticles. *Water Res.* **2011**, *45* (5), 1961–1972.
865 <https://doi.org/10.1016/j.watres.2011.01.004>.

866 (110) Arias-Paić, M. S.; Korak, J. A. Forward Osmosis for Ion Exchange Waste Brine Management.
867 *Environ. Sci. Technol. Lett.* **2020**, *7* (2), 111–117. <https://doi.org/10.1021/acs.estlett.9b00733>.

868 (111) Bergquist, A. M.; Choe, J. K.; Strathmann, T. J.; Werth, C. J. Evaluation of a Hybrid Ion
869 Exchange-Catalyst Treatment Technology for Nitrate Removal from Drinking Water. *Water Res.*
870 **2016**, *96*, 177–187. <https://doi.org/10.1016/j.watres.2016.03.054>.

871 (112) Jones, D. R. Improved Spectrophotometric Method for the Determination of Low Levels of
872 Bromide. *Anal. Chim. Acta* **1993**, *271* (2), 315–321. [https://doi.org/10.1016/0003-2670\(93\)80061-](https://doi.org/10.1016/0003-2670(93)80061-O)
873 O.

- 874 (113) De Geyter, N.; Morent, R.; Leys, C.; Gengembre, L.; Payen, E. Treatment of Polymer Films with a
875 Dielectric Barrier Discharge in Air, Helium and Argon at Medium Pressure. *Surf. Coatings*
876 *Technol.* **2007**, *201* (16–17), 7066–7075. <https://doi.org/10.1016/j.surfcoat.2007.01.008>.
- 877 (114) Jiang, J.; Han, J.; Zhang, X. Nonhalogenated Aromatic DBPs in Drinking Water Chlorination: A
878 Gap between NOM and Halogenated Aromatic DBPs. *Environ. Sci. Technol.* **2020**, *54* (3), 1646–
879 1656. <https://doi.org/10.1021/acs.est.9b06403>.
- 880 (115) Hasegawa, K.; Neta, P. Rate Constants and Mechanisms of Reaction of Chloride (Cl₂⁻) Radicals.
881 *J. Phys. Chem.* **1978**, *82* (8), 854–857. <https://doi.org/10.1021/j100497a003>.
- 882 (116) Lei, Y.; Lei, X.; Yu, Y.; Li, K.; Li, Z.; Cheng, S.; Ouyang, G.; Yang, X. Rate Constants and
883 Mechanisms for Reactions of Bromine Radicals with Trace Organic Contaminants. *Environ. Sci.*
884 *Technol.* **2021**, *55* (15), 10502–10513. <https://doi.org/10.1021/acs.est.1c02313>.
- 885 (117) Kemsley, K.; Moore, J. S.; Phillip, G. O.; Sosnowski, A. Reaction of Radical Probes with
886 Substituted Phenols as Models for the Investigation of Tyrosine in Aldolase and Chemically
887 Modified Aldolase. *Acta Vitaminol. Enzym.* **1974**, *28* (6), 263–267.
- 888 (118) Lei, Y.; Cheng, S.; Luo, N.; Yang, X.; An, T. Rate Constants and Mechanisms of the Reactions of
889 Cl[•] and Cl₂^{•-} with Trace Organic Contaminants. *Environ. Sci. Technol.* **2019**.
890 <https://doi.org/10.1021/acs.est.9b02462>.
- 891 (119) Barazesh, J. M.; Prasse, C.; Sedlak, D. L. Electrochemical Transformation of Trace Organic
892 Contaminants in the Presence of Halide and Carbonate Ions. *Environ. Sci. Technol.* **2016**, *50* (18),
893 10143–10152. <https://doi.org/10.1021/acs.est.6b02232>.
- 894 (120) Mertens, R.; von Sonntag, C. Photolysis ($\lambda=254$ nm) of Tetrachloroethene in Aqueous Solutions.
895 *J. Photochem. Photobiol. A Chem.* **1995**, *85* (1–2), 1–9. <https://doi.org/10.1016/1010->
896 [6030\(94\)03903-8](https://doi.org/10.1016/1010-6030(94)03903-8).

- 897 (121) Huie, R. E.; Clifton, C. L.; Neta, P. Electron Transfer Reaction Rates and Equilibria of the
898 Carbonate and Sulfate Radical Anions. *Radiat. Phys. Chem. Int. J. Radiat. Appl. Instrum., Part C*
899 **1991**, 38 (5), 477–481.
- 900 (122) Jiang, P.-Y.; Katsumura, Y.; Nagaishi, R.; Domae, M.; Ishikawa, K.; Ishigure, K.; Yoshida, Y.
901 Pulse Radiolysis Study of Concentrated Sulfuric Acid Solutions. *J. Chem. Soc. Faraday Trans.*
902 **1992**, 88 (22), 3319–3322. <https://doi.org/10.1039/FT9928803319>.
- 903 (123) Katsumura, Y.; Jiang, P. Y.; Nagaishi, R.; Oishi, T.; Ishigure, K.; Yoshida, Y. Pulse Radiolysis
904 Study of Aqueous Nitric Acid Solutions. Formation Mechanism, Yield, and Reactivity of NO₃
905 Radical. *J. Phys. Chem.* **1991**, 95 (11), 4435–4439. <https://doi.org/10.1021/j100164a050>.
- 906 (124) Buxton, G. V.; Elliot, A. J. Rate Constant for Reaction of Hydroxyl Radicals with Bicarbonate
907 Ions. *Int. J. Radiat. Appl. Instrumentation. Part* **1986**, 27 (3), 241–243.
908 [https://doi.org/10.1016/1359-0197\(86\)90059-7](https://doi.org/10.1016/1359-0197(86)90059-7).
- 909 (125) Westerhoff, P.; Mezyk, S. P.; Cooper, W. J.; Minakata, D. Electron Pulse Radiolysis
910 Determination of Hydroxyl Radical Rate Constants with Suwannee River Fulvic Acid and Other
911 Dissolved Organic Matter Isolates. *Environ. Sci. Technol.* **2007**, 41 (13), 4640–4646.
912 <https://doi.org/10.1021/es062529n>.
- 913 (126) Chen, R.; Avotins, Y.; Freeman, G. R. Solvent Effects on Reactivity of Solvated Electrons with
914 Ions in Isobutanol/Water Mixed Solvents. *Can. J. Chem.* **1994**, 72 (4), 1083–1093.
915 <https://doi.org/10.1016/j.jiec.2008.03.002>.
- 916 (127) Thomas, J. K.; Gordon, S.; Hart, E. J. The Rates of Reaction of the Hydrated Electron in Aqueous
917 Inorganic Solutions. *J. Phys. Chem.* **1964**, 68 (6), 1524–1527.
918 <https://doi.org/10.1021/j100788a043>.
- 919 (128) Nash, K.; Mulac, W.; Noon, M.; Fried, S.; Sullivan, J. C. Pulse Radiolysis Studies of U(VI)

- 920 Complexes in Aqueous Media. *J. Inorg. Nucl. Chem.* **1981**, *43* (5), 897–899.
921 [https://doi.org/10.1016/0022-1902\(81\)80146-7](https://doi.org/10.1016/0022-1902(81)80146-7).
- 922 (129) Huang, Y. C.; Rao, A.; Huang, S. J.; Chang, C. Y.; Drechsler, M.; Knaus, J.; Chan, J. C. C.;
923 Raiteri, P.; Gale, J. D.; Gebauer, D. Uncovering the Role of Bicarbonate in Calcium Carbonate
924 Formation at Near-Neutral pH. *Angew. Chemie - Int. Ed.* **2021**, *60* (30), 16707–16713.
925 <https://doi.org/10.1002/anie.202104002>.
- 926 (130) Van Driessche, A. E. S.; Stawski, T. M.; Kellermeier, M. Calcium Sulfate Precipitation Pathways
927 in Natural and Engineered Environments. *Chem. Geol.* **2019**, *530*, 119274.
928 <https://doi.org/10.1016/j.chemgeo.2019.119274>.
- 929 (131) Case, D. H.; Wang, F.; Giammar, D. E. Precipitation of Magnesium Carbonates as a Function of
930 Temperature, Solution Composition, and Presence of a Silicate Mineral Substrate. *Environ. Eng.*
931 *Sci.* **2011**, *28* (12), 881–889. <https://doi.org/10.1089/ees.2010.0341>.
- 932 (132) American Public Health Association. *Standard Methods for the Examination of Water and*
933 *Wastewater*; 1998.
- 934 (133) Pearse, R. W. B.; Gaydon, A. G. *The Identification of Molecular Spectra*; London Chapman &
935 Hall LTD, 1941.
- 936 (134) National Institute of Standards and Technology. Atomic Spectra Database Lines Data
937 https://physics.nist.gov/PhysRefData/ASD/lines_form.html (accessed 2023-07-23).
- 938 (135) Hong, Y. J.; Nam, C. J.; Song, K. B.; Cho, G. S.; Uhm, H. S.; Choi, D. I.; Choi, E. H.
939 Measurement of Hydroxyl Radical Density Generated from the Atmospheric Pressure Bioplasma
940 Jet. *J. Instrum.* **2012**, *7* (3). <https://doi.org/10.1088/1748-0221/7/03/C03046>.
- 941 (136) Zhang, D. J.; Cai, Y.; Chen, M. L.; Yu, Y. L.; Wang, J. H. Dielectric Barrier Discharge-Optical
942 Emission Spectrometry for the Simultaneous Determination of Halogens. *J. Anal. At. Spectrom.*

- 943 **2016**, *31* (2), 398–405. <https://doi.org/10.1039/c5ja00266d>.
- 944 (137) Ashton, L.; Buxton, G. V.; Stuart, C. R. Temperature Dependence of the Rate of Reaction of OH
945 with Some Aromatic Compounds in Aqueous Solution Evidence for the Formation of a π -
946 Complex Intermediate? *J. Chem. Soc. Faraday Trans.* **1995**, *91* (11), 1631–1633.
947 [https://doi.org/10.1016/s0082-0784\(00\)80664-5](https://doi.org/10.1016/s0082-0784(00)80664-5).
- 948 (138) Anderson, R. F.; Patel, K. B.; Stratford, M. R. L. Radical Spectra and Product Distribution
949 Following Electrophilic Attack by the OH. Radical on 4-Hydroxybenzoic Acid and Subsequent
950 Oxidation. *J. Chem. Soc. Faraday Trans. 1 Phys. Chem. Condens. Phases* **1987**, *83* (10), 3177–
951 3187. <https://doi.org/10.1039/F19878303177>.
- 952 (139) Anbar, M.; Alfassi, Z. B.; Bregman-Reisler, H. Hydrated Electron Reactions in View of Their
953 Temperature Dependence. *J. Am. Chem. Soc.* **1967**, *89* (5), 1263–1264.
- 954 (140) Neta, P.; Schuler, R. H. Effect of Ionic Dissociation of Organic Compounds on Their Rate of
955 Reaction with Hydrogen Atoms. *J. Phys. Chem.* **1972**, *76* (19), 2673–2679.
- 956 (141) Neta, P.; Dorfman, L. M. Pulse-Radiolysis Studies. XIV. Rate Constants for the Reactions of
957 Hydrogen Atoms with Aromatic Compounds in Aqueous Solution. *J. Phys. Chem.* **1969**, *73* (2),
958 413–417. <https://doi.org/10.1021/j100722a025>.
- 959 (142) Li, Y.; Song, W.; Fu, W.; Tsang, D. C. W.; Yang, X. The Roles of Halides in the Acetaminophen
960 Degradation by UV/H₂O₂ Treatment: Kinetics, Mechanisms, and Products Analysis. *Chem. Eng. J.*
961 **2015**, *271*, 214–222. <https://doi.org/10.1016/j.cej.2015.02.090>.
- 962 (143) Rebenne, L. M.; Gonzalez, A. C.; Olson, T. M. Aqueous Chlorination Kinetics and Mechanism of
963 Substituted Dihydroxybenzenes. *Environ. Sci. Technol.* **1996**, *30* (7), 2235–2242.
964 <https://doi.org/10.1021/es950607t>.
- 965 (144) Korshin, G. V. Chlorine Based Oxidants for Water Purification and Disinfection. In *Aquatic Redox*

- 966 *Chemistry* **2011**, 1071, 223–245. <https://doi.org/10.1021/bk-2011-1071.ch011>.
- 967 (145) Sivey, J. D.; Bickley, M. A.; Victor, D. A. Contributions of BrCl, Br₂, BrOCl, Br₂O, and HOBr to
968 Regiospecific Bromination Rates of Anisole and Bromoanisoles in Aqueous Solution. *Environ.*
969 *Sci. Technol.* **2015**, 49 (8), 4937–4945. <https://doi.org/10.1021/acs.est.5b00205>.
- 970 (146) Liu, T.; Xiao, S.; Li, N.; Chen, J.; Xu, Y.; Yin, W.; Zhou, X.; Huang, C. H.; Zhang, Y. Selective
971 Transformation of Micropollutants in Saline Wastewater by Peracetic Acid: The Overlooked
972 Brominating Agents. *Environ. Sci. Technol.* **2023**. <https://doi.org/10.1021/acs.est.3c00835>.
- 973 (147) Perlmutter-Hayman, B.; Weissmann, Y. The Oxidation of 2-Propanol by Bromine and by
974 Hypobromous Acid in Aqueous Solution. *J. Am. Chem. Soc.* **1969**, 91 (3), 668–672.
975 <https://doi.org/10.1021/ja01031a025>.
- 976 (148) Zhang, B.; Fang, Z.; Wang, S.; Shi, X.; Guo, B.; Gao, J.; Wang, D.; Zong, W. Effect of Bromide
977 on Molecular Transformation of Dissolved Effluent Organic Matter during Ozonation, UV/H₂O₂,
978 UV/Persulfate, and UV/Chlorine Treatments. *Sci. Total Environ.* **2022**, 811, 152328.
979 <https://doi.org/10.1016/j.scitotenv.2021.152328>.
- 980 (149) Shu, Z.; Wang, J.; Liu, H.; Liu, C. Improvement of Bromide Ions on the Degradation of
981 Sulfamerazine by Horseradish Peroxidase-H₂O₂ System and Its Interaction Mechanisms. *Chem.*
982 *Eng. J.* **2022**, 428, 131132. <https://doi.org/10.1016/j.cej.2021.131132>.
- 983 (150) Oum, K. W.; Lakin, M. J.; DeHaan, D. O.; Brauers, T.; Finlayson-Pitts, B. J. Formation of
984 Molecular Chlorine from the Photolysis of Ozone and Aqueous Sea-Salt Particles. *Science*. **1998**,
985 279 (5347), 74–77. <https://doi.org/10.1126/science.279.5347.74>.
- 986 (151) George, I. J.; Abbatt, J. P. D. Heterogeneous Oxidation of Atmospheric Aerosol Particles by Gas-
987 Phase Radicals. *Nat. Chem.* **2010**, 2 (9), 713–722. <https://doi.org/10.1038/nchem.806>.
- 988 (152) Enami, S.; Hoffmann, M. R.; Colussi, A. J. Halogen Radical Chemistry at Aqueous Interfaces. *J.*

- 989 *Phys. Chem. A* **2016**, *120* (31), 6242–6248. <https://doi.org/10.1021/acs.jpca.6b04219>.
- 990 (153) Amphlett, C. B.; Adams, G. E.; Michael, B. D. Pulse Radiolysis Studies of Deaerated Aqueous
991 Salicylate Solutions. In *Radiation Chemistry* **1968**, 231–250. [https://doi.org/10.1021/ba-1968-](https://doi.org/10.1021/ba-1968-0081.ch016)
992 0081.ch016.
- 993 (154) Bisby, R. H.; Tabassum, N. Properties of the Radicals Formed by One-Electron Oxidation of
994 Acetaminophen-A Pulse Radiolysis Study. *Biochem. Pharmacol.* **1988**, *37* (14), 2731–2738.
995 [https://doi.org/10.1016/0006-2952\(88\)90035-4](https://doi.org/10.1016/0006-2952(88)90035-4).
- 996 (155) Mezyk, S. P.; Neubauer, T. J.; Cooper, W. J.; Peller, J. R. Free-Radical-Induced Oxidative and
997 Reductive Degradation of Sulfa Drugs in Water: Absolute Kinetics and Efficiencies of Hydroxyl
998 Radical and Hydrated Electron Reactions. *J. Phys. Chem. A* **2007**, *111* (37), 9019–9024.
999 <https://doi.org/10.1021/jp073990k>.
- 1000 (156) Prutz, W. A.; Land, E. J. Chemiluminescent Reactions after Pulse Radiolysis of Aqueous Dye
1001 Solutions. Absolute Yields. *J. Phys. Chem.* **1974**, *78* (13), 1251–1253.
- 1002 (157) Wojnárovits, L.; Tóth, T.; Takács, E. Rate Constants of Carbonate Radical Anion Reactions with
1003 Molecules of Environmental Interest in Aqueous Solution: A Review. *Sci. Total Environ.* **2020**,
1004 *717*. <https://doi.org/10.1016/j.scitotenv.2020.137219>.
- 1005 (158) Olszowy, H. A.; Rossiter, J.; Hegarty, J.; Geoghegan, P.; Haswell-Elkins, M. Background Levels
1006 of Bromide in Human Blood. *J. Anal. Toxicol.* **1998**, *22* (3), 225–230.
1007 <https://doi.org/10.1093/jat/22.3.225>.
- 1008 (159) Kaushik, N.; Lee, S. J.; Choi, T. G.; Baik, K. Y.; Uhm, H. S.; Kim, C. H.; Kaushik, N. K.; Choi, E.
1009 H. Non-Thermal Plasma with 2-Deoxy-D-Glucose Synergistically Induces Cell Death by
1010 Targeting Glycolysis in Blood Cancer Cells. *Sci. Rep.* **2015**, *5*, 1–11.
1011 <https://doi.org/10.1038/srep08726>.

- 1012 (160) Scholtz, V.; Pazlarova, J.; Souskova, H.; Khun, J.; Julak, J. Nonthermal Plasma - A Tool for
1013 Decontamination and Disinfection. *Biotechnol. Adv.* **2015**, *33* (6), 1108–1119.
1014 <https://doi.org/10.1016/j.biotechadv.2015.01.002>.
- 1015 (161) Guesmi, A.; Cherif, M. M.; Baaloudj, O.; Kenfoud, H.; Badawi, A. K.; Elfalleh, W.; Hamadi, N.
1016 Ben; Khezami, L.; Assadi, A. A. Disinfection of Corona and Myriad Viruses in Water by Non-
1017 Thermal Plasma: A Review. *Environ. Sci. Pollut. Res.* **2022**, *29* (37), 55321–55335.
1018 <https://doi.org/10.1007/s11356-022-21160-7>.
- 1019 (162) Patange, A.; Boehm, D.; Giltrap, M.; Lu, P.; Cullen, P. J.; Bourke, P. Assessment of the
1020 Disinfection Capacity and Eco-Toxicological Impact of Atmospheric Cold Plasma for Treatment
1021 of Food Industry Effluents. *Sci. Total Environ.* **2018**, *631–632*, 298–307.
1022 <https://doi.org/10.1016/j.scitotenv.2018.02.269>.
- 1023 (163) Kondeti, V. S. S. K.; Phan, C. Q.; Wende, K.; Jablonowski, H.; Gangal, U.; Granick, J. L.; Hunter,
1024 R. C.; Bruggeman, P. J. Long-Lived and Short-Lived Reactive Species Produced by a Cold
1025 Atmospheric Pressure Plasma Jet for the Inactivation of *Pseudomonas Aeruginosa* and
1026 *Staphylococcus Aureus*. *Free Radic. Biol. Med.* **2018**, *124*, 275–287.
1027 <https://doi.org/10.1016/j.freeradbiomed.2018.05.083>.
- 1028 (164) Hua, G.; Reckhow, D. A. Comparison of Disinfection Byproduct Formation from Chlorine and
1029 Alternative Disinfectants. *Water Res.* **2007**, *41* (8), 1667–1678.
1030 <https://doi.org/10.1016/j.watres.2007.01.032>.
- 1031 (165) Hua, G.; Reckhow, D. A. Evaluation of Bromine Substitution Factors of DBPs during
1032 Chlorination and Chloramination. *Water Res.* **2012**, *46* (13), 4208–4216.
1033 <https://doi.org/10.1016/j.watres.2012.05.031>.
- 1034 (166) Silvio, C.; Kohn, T.; Mac, M.; Real, F. J.; Wirz, J.; Gunten, U. von. Photosensitizer Method to
1035 Determine Rate Constants for the Reaction of Carbonate Radical with Organic Compounds.

1036 *Environ. Sci. Technol.* **2005**, 39 (23), 9182–9188. <https://doi.org/10.1021/es051236b>.

1037 (167) Bolton, J. R.; Bircher, K. G.; Tumas, W.; Tolman, C. A. Figures-of-Merit for the Technical
1038 Development and Application of Advanced Oxidation Technologies for Both Electric- and Solar-
1039 Driven Systems. *Pure Appl. Chem.* **2001**, 73 (4), 627–637.
1040 <https://doi.org/10.1351/pac200173040627>.

1041